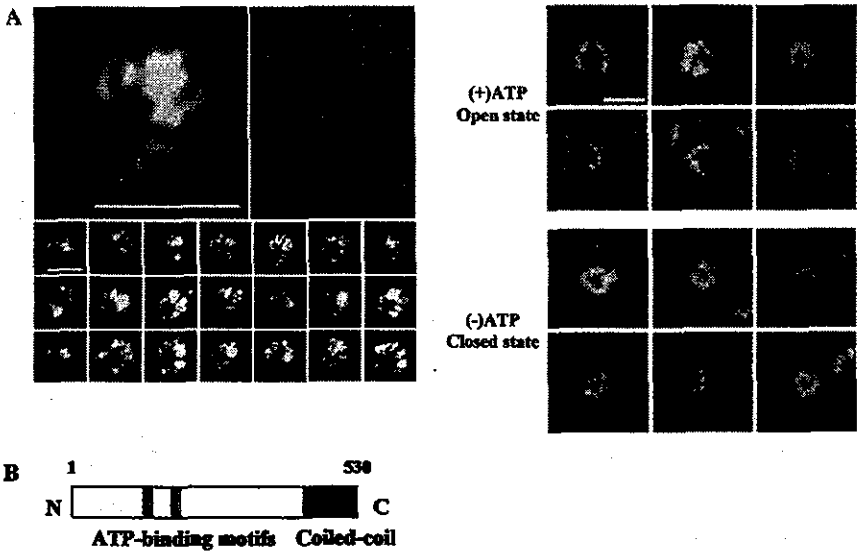


Fig. 1. A grapple-like oligomeric structure of Aip2p/Dld2p. (A) Left panels: purified hexahistidine-tagged oligomeric Aip2p/Dld2p (100 μg ml$^{-1}$) was used as a specimen for low angle shadowing electron microscopy. Scale bars are 10 nm. Right panels: negative staining of oligomeric Aip2p/Dld2p in the "open state" and "closed state." In the presence of ATP, oligomeric Aip2p/Dld2p opens its opening ((+)ATP) and without ATP the opening is closed ((−)ATP). Scale bar is 10 nm. (B) Schematic representation of the structure of YDL178W [2] encoding Aip2p/Dld2p. Two ATP-binding Walker type B motifs (ZZZZD, where Z is a hydrophobic residue) [11] locate at amino acid residues from 142 to 146 and 189 to 193 (hatched), and a coiled-coil domain locates in its C-terminal 100 amino acid residues (filled) [12].

(ZZZZD, where Z is a hydrophobic residue) [11] located at amino acid residues from 142 to 146 and 189 to 193, which are conserved among several $Mg^{2+}$-nucleotide binding proteins (Fig. 1B).

Gel filtration chromatography was then performed in order to determine the number of Aip2p/Dld2p monomers present in the oligomeric complex. Oligomeric Aip2p/Dld2p eluted as a single peak with an apparent molecular weight of ~700 kDa (Fig. 2A). Given that the molecular weight of Aip2p/Dld2p in the monomeric form was about ~60 kDa [1], it is apparent that Aip2p/Dld2p forms an oligomeric structure consisting of 10–12 subunits. Secondary structure prediction [12] indicated that Aip2p/Dld2p contains a coiled-coil domain in its C-terminal region (Fig. 1B). To determine the functional significance of this region in relation to oligomerization, coiled-coil region-deleted recombinant Aip2p/Dld2p was expressed and purified from yeast cells. As shown in Fig. 2B, C-terminal-truncated Aip2p/Dld2p eluted at an apparent molecular weight of ~60 kDa, indicating that Aip2p/Dld2p oligomerization occurs via the C-terminal coiled-coil region. Next, the protease susceptibility assay was employed to examine the conformation modifying activity of the coiled-coil domain-deleted monomeric form of Aip2p/Dld2p. This truncated monomeric form of Aip2p/Dld2p did not possess F-actin conformation modifying activity, as suggested by the result that its trypsin susceptibility was not affected even in the presence of ATP (Fig. 2C).

In addition to the aforementioned indirect biochemical analyses suggesting that oligomeric Aip2p/Dld2p possesses F-actin conformation modifying activity, more direct evidence of this activity was sought through the use of low angle rotary shadowing [9]. Following incubation of rabbit muscle F-actin with oligomeric Aip2p/Dld2p in the presence of ATP (open state of Aip2p/Dld2p), oligomeric Aip2p/Dld2p bound the F-actin fiber within the opening (Fig. 3A, (+)ATP), whereas in the absence of ATP (closed state of Aip2p/Dld2p), given that the opening was closed, no binding was observed (Fig. 3A, (−)ATP). Previously, we reported that incubation with Aip2p/Dld2p facilitated the formation of the circular form of F-actin in vitro, which exhibited an aberrant trypsin susceptibility [1]. However, the radius of this circular F-actin was 2–4 μm on average and was not detectable under the electron microscope at higher magnification (100,000×) used in this study. Consistent with these results, oligomeric Aip2p/Dld2p increased the trypsin susceptibility of F-actin in the presence of ATP (Fig. 3B, (+)ATP). Use of the non-hydrolyzable ATP analogue AMP–PNP yielded similar results to those observed with ATP (Fig. 3B, (+)AMP–PNP), whereas the use of ADP failed to alter the trypsin susceptibility of F-actin (Fig. 3B, (+)ADP). These data suggested that ATP binding rather than ATP hydrolysis is required for the protein conformation modifying reaction of oligomeric Aip2p/Dld2p.

The trypsin susceptibility assay was further applied to isolate the F-actin conformation modifying activity in yeast cells in vivo. Several steps consisting of ion exchange chromatography followed by affinity chromatography with ATP–agarose facilitated the purification to homogeneity of endogenous Aip2p/Dld2p, of which the identity was confirmed by amino acid sequence

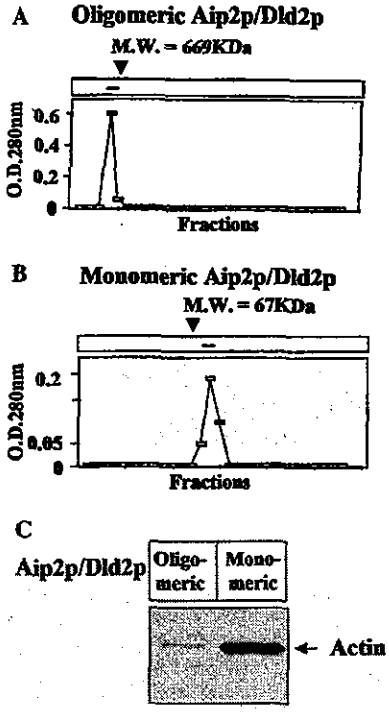


Fig. 2. Oligomeric Aip2p/Dld2p exhibits F-actin conformation modifying activity. (A) Gel filtration chromatography (Superdex 200 column, Amersham *BioSciences, Smart system*) was performed with purified hexahistidine-tagged full-length Aip2p/Dld2p in oligomeric form. Thyroglobulin (molecular weight (MW) = 669 kDa) was used as a marker protein. (B) The C-terminal coiled-coil region-truncated Aip2p/Dld2p eluted as a monomeric protein. Bovine serum albumin (MW = 67 kDa) was used as a marker protein. (C) The coiled-coil region-truncated monomeric Aip2p/Dld2p possesses no protein conformation modifying activity. Two micromolar of rabbit muscle actin (Molecular Probes) was polymerized in the high salt buffer (10 mM Tris–Cl, pH 8.0, 100 mM KCl, and 2 mM $MgCl_2$) at 37 °C for 2 h. Oligomeric and monomeric forms of Aip2p/Dld2p were purified and incubated with the polymerized rabbit muscle actin in the presence of 1 mM ATP and the trypsin susceptibility assay was performed.

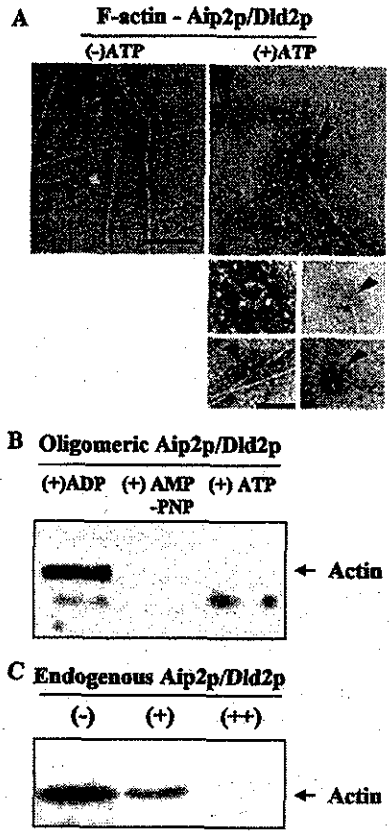


Fig. 3. F-actin binding and conformation modifying activity of oligomeric Aip2p/Dld2p are ATP-dependent. (A) Two hundred micrograms of polymerized rabbit muscle actin (see legend to Fig. 2C) was incubated with or without 500 μg of oligomeric Aip2p/Dld2p in the presence or absence of 1 mM ATP and then examined by negative staining (100,000×). Scale bars are 20 nm. In the presence of ATP, oligomeric Aip2p/Dld2p (arrowheads) binds to F-actin in the opening. (B) The same reaction mixture was subjected to the trypsin susceptibility assay. F-actin (200 ng) and oligomeric Aip2p/Dld2p (500 ng) were incubated in buffer E with 1 mM ATP ((+)ATP), 1 mM AMP–PNP ((+)AMP–PNP) or 1 mM ADP ((+)ADP). In the presence of ATP ((+)ATP) or AMP–PNP ((+)AMP–PNP), oligomeric Aip2p/Dld2p modifies the trypsin susceptibility of F-actin. Endogenous Aip2p/Dld2p purified from *S. cerevisiae* exhibits actin conformation modifying activity. (C) Endogenous Aip2p/Dld2p (–) represents the trypsin-protected control band. (+)/(++) refers to 300/500 ng of endogenous Aip2p/Dld2p. Protected bands were detected by Western blotting using polyclonal antibodies against actin and visualized with ECL-plus. Endogenous Aip2p/Dld2p alters the trypsin susceptibility of actin in a dose-dependent manner.

analysis (see Materials and methods). Low concentrations of trypsin did not digest actin (Fig. 3C, (–)). However, when endogenous Aip2p/Dld2p purified from *S. cerevisiae* was added and incubated for 15 min at 30 °C, the previously protected band decreased in intensity depending on the amount of extract added (Fig. 3C, (+) and (++)). Given the fact that truncated monomeric form of Aip2p/Dld2p does not possess F-actin conformation modifying activity, the purified Aip2p/Dld2p is likely to be an oligomeric form.

## Discussion

### *Oligomeric Aip2p/Dld2p forms an unusual "grapple-like" structure*

Given that structural analysis can provide details concerning the molecular profiles of targets, the ultrastructure of oligomeric Aip2p/Dld2p was visualized directly using low angle rotary shadowing electron microscopy. This revealed a grapple-like oligomeric structure of ~10 nm in diameter within the opening. In the presence of ATP, oligomeric Aip2p/Dld2p bound F-actin in the opening through its unique "grapple-like" structure, which is quite unprecedented. F-actin entered and was caught in the grapple-shaped opening, where its conformation was modified in the presence of ATP. On the other hand, in the absence of ATP or in the presence

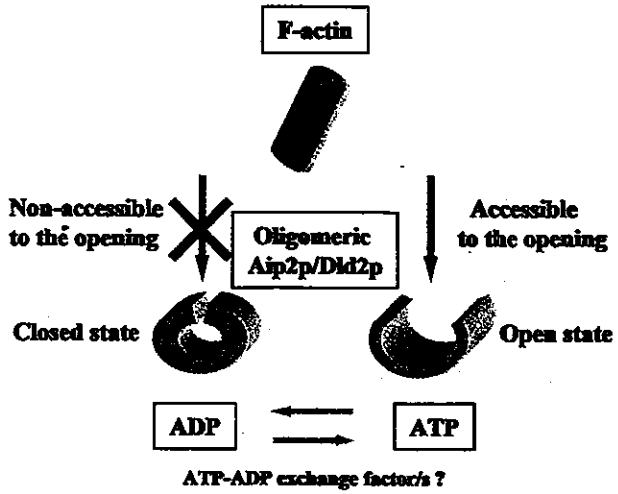


Fig. 4. The ATP-dependent open and closed state model of oligomeric Aip2p/Dld2p. ATP-bound oligomeric Aip2p/Dld2p exhibits a protein conformation modifying activity (open state), whereas F-actin is unable to penetrate ATP-unbound oligomeric Aip2p/Dld2p (closed state).

of ADP, the opening was closed, and thus F-actin could not enter the opening (Fig. 4). Consistent with this observation, monomeric Aip2p/Dld2p with a C-terminal coiled-coil region-truncation failed to exhibit the protein conformation modifying activity.

The structures and functions of Hsp70 family proteins and chaperonins have been extensively investigated [13,14]. DnaK binds short peptides bearing a core of hydrophobic residues to its cleft with a lid, the opening and closing of which is mediated via the ATPase domain [15]. Group I chaperonins generally form homoheptameric rings stacked back-to-back to yield a cylinder possessing two central cavities. GroEL, with conserved hydrophobic residues that are aligned along the cylinder opening on the apical domains, recognizes and binds hydrophobic surfaces of nonnative proteins [16]. ATP-binding and the dome-shaped cofactor, GroES, displace the bound substrate from within the GroEL cavity, where folding is facilitated by preventing aggregation [17]. Group II chaperonins, GimC/prefoldin, TRiC/CCT, and thermosome are not homologous to Group I chaperonins but share a similar overall architecture. They form homo-oligomeric rings of 8–9 subunits and function without a GroES-like capping cofactor [15,18]. They apparently rely on α-helical extensions of their apical domains that are thought to mediate opening and closing of their folding chamber and have a "built-in" lid.

While these chaperonins are composed of similar oligomeric structures within the central cavity, oligomeric Aip2p/Dld2p is clearly distinct with a grapple-like structure of 10–12 subunits that can modify the conformation of substrate. When interactions between the conventional chaperonins and long fibrous substrates such as F-actin are considered, oligomeric Aip2p/Dld2p may outperform the ring- or cylinder-shaped conventional chaperonins, since with the latter, either end has to be dragged in and then passed through the central cavity all the way. In contrast, a grapple-like structure in the "open state" is able to bind targets, such long fibers, directly at any point, even in the middle.

### *Oligomeric Aip2p/Dld2p exhibits an ATP-dependent F-actin conformation modifying activity*

It was found that oligomeric Aip2p/Dld2p exhibited an F-actin conformation modifying activity, which is regulated by the binding of ATP to oligomeric Aip2p/Dld2p. It has been well documented that the activity of hsp70 proteins is regulated by two co-chaperones, DnaJ homologues that stimulate ATP hydrolysis [19,20], and GrpE that mediates the ATP–ADP exchange reaction [21,22]. Although the reaction mechanism associated with oligomeric Aip2p/Dld2p is clearly distinct from hsp70, we are tempted to speculate that a similar factor/s may function as co-chaperone/s to regulate ATP-hydrolysis or ATP–ADP exchange in the protein conformation modification cycle. Actually, the protein conformation modifying activity is regulated by the binding of ATP to oligomeric Aip2p/Dld2p, but not by ATP hydrolysis according to the current experimental result with non-hydrolyzable ATP analogue, AMP–PNP. Consistent with this notion, partially purified Aip2p/Dld2p at the log phase possessed higher protein conformation modifying activity and ATP-binding capacity than those of Aip2p/Dld2p purified at the stationary phase, suggesting the presence of a cofactor/s that may provide ATP to Aip2p/Dld2p (Hachiya et al., unpublished data).

Finally, it is important to clarify if the oligomeric Aip2p/Dld2p exclusively binds and modifies F-action conformation. Although it is very preliminary, our data suggested that the oligomeric Aip2p/Dld2p also bound and modified the conformation of DNase I, the mature form of invertase, mitochondrial SOD, and heavy meromyosin, as determined by the trypsin susceptibility assay (data not shown). Clearly, more detailed examination especially on its substrate specificity in vivo has yet to be done.

These data may support the notion that the oligomeric Aip2p/Dld2p may belong to an unusual class of molecular chaperones, which exhibits the unique grapple-like structure with an ATP-dependent opening. Whether such activity is exceptional or forms a novel class of molecular chaperones remains to be determined.

## Acknowledgments

We are indebted to G. Schatz, S.B. Prusiner, K. Mihara, and R. Scheckman for critical discussions and to I. Wada, N. Hoogenraad, M. Ryan, and A. Asano for helpful comments. We are also grateful to Y.

Kozuka, K. Ihara, S. Yoshioka, M. Yamada, K. Watanabe, E.A. Nannri, and K. Ishibashi for technical assistance. This work was supported in part by grants from the Ministry of Health, Labor and Welfare of Japan, Exploratory Research for Advanced Technology (ERATO) and Core Research for Evolutional Science and Technology (CREST) of the Japan Science Technology Corporation (JST), Health and Labour Sciences Research Grants, Research on Advanced Medical Technology, nano-001, the Ministry of Health, Labour and Welfare of Japan, and the Naito Foundation.

## References

[1] N.S. Hachiya, Y. Sakasegawa, A. Jozuka, S. Tsukita, K. Kaneko, Interaction of D-lactate dehydrogenase protein 2 (Dld2p) with F-actin: implication for an alternative function of Dld2p, Biochem. Biophys. Res. Commun. 319 (2004) 78–82.

[2] D.C. Amberg, E. Basart, D. Botstein, Defining protein interactions with yeast actin in vivo, Nat. Struct. Biol. 2 (1995) 28–35.

[3] A. Chelstowska, Z. Liu, Y. Jia, D. Amberg, R.A. Butow, Signalling between mitochondria and the nucleus regulates the expression of a new D-lactate dehydrogenase activity in yeast, Yeast 15 (1999) 1377–1391.

[4] M.J. Flick, S.F. Konieczny, Identification of putative mammalian D-lactate dehydrogenase enzymes, Biochem. Biophys. Res. Commun. 295 (2002) 910–916.

[5] B. Schwikowski, P. Uetz, S. Fields, A network of protein–protein interactions in yeast, Nat. Biotechnol. 18 (2000) 1257–1261.

[6] N. Hachiya, R. Alam, Y. Sakasegawa, M. Sakaguchi, K. Mihara, T. Omura, A mitochondrial import factor purified from rat liver cytosol is an ATP-dependent conformational modulator for precursor proteins, EMBO J. 12 (1993) 1579–1586.

[7] N. Hachiya, T. Komiya, R. Alam, J. Iwahashi, M. Sakaguchi, T. Omura, K. Mihara, MSF, a novel cytoplasmic chaperone which functions in precursor targeting to mitochondria, EMBO J. 13 (1994) 5146–5154.

[8] N. Hachiya, K. Mihara, K. Suda, M. Horst, G. Schatz, T. Lithgow, Reconstitution of the initial steps of mitochondrial protein import, Nature 376 (1995) 705–709.

[9] S. Tsukita, Desmocalmin: a calmodulin-binding high molecular weight protein isolated from desmosomes, J. Cell Biol. 101 (1985) 2070–2080.

[10] Y. Nonomura, E. Katayama, S. Ebashi, Effect of phosphates on the structure of the actin filament, J. Biochem. (Tokyo) 78 (1975) 1101–1104.

[11] J.E. Walker, M. Saraste, M.J. Runswick, N.J. Gay, Distantly related sequences in the alpha- and beta-subunits of ATP synthase, myosin, kinases and other ATP-requiring enzymes and a common nucleotide binding fold, EMBO J. 1 (1982) 945–951.

[12] A. Lupas, M. Van Dyke, J. Stock, Predicting coiled coils from protein sequences, Science 252 (1991) 1162–1164.

[13] F.U. Hartl, Molecular chaperones in cellular protein folding, Nature 381 (1996) 571–580.

[14] S. Walter, J. Buchner, Molecular chaperones—cellular machines for protein folding, Angew. Chem. Int. Ed. Engl. 41 (2002) 1098–1113.

[15] M.P. Mayer, H. Schroder, S. Rudiger, K. Paal, T. Laufen, B. Bukau, Multistep mechanism of substrate binding determines chaperone activity of Hsp70, Nat. Struct. Biol. 7 (2000) 586–593.

[16] W.A. Houry, Mechanism of substrate recognition by the chaperonin GroEL, Biochem. Cell. Biol. 79 (2001) 569–577.

[17] J.S. Weissman, C.M. Hohl, O. Kovalenko, Y. Kashi, S. Chen, K. Braig, H.R. Saibil, W.A. Fenton, A.L. Horwich, Mechanism of GroEL action: productive release of polypeptide from a sequestered position under GroES, Cell 83 (1995) 577–587.

[18] A.S. Meyer, J.R. Gillespie, D. Walther, I.S. Millet, S. Doniach, J. Frydman, Closing the folding chamber of the eukaryotic chaperonin requires the transition state of ATP hydrolysis, Cell 113 (2003) 369–381.

[19] T. Laufen, M.P. Mayer, C. Beisel, D. Klostermeier, A. Mogk, J. Reinstein, B. Bukau, Mechanism of regulation of hsp70 chaperones by DnaJ cochaperones, Proc. Natl. Acad. Sci. USA 96 (1999) 5452–5457.

[20] R. Russell, A. Wali Karzai, A.F. Mehl, R. McMacken, DnaJ dramatically stimulates ATP hydrolysis by DnaK: insight into targeting of Hsp70 proteins to polypeptide substrates, Biochemistry 38 (1999) 4165–4176.

[21] Y. Groemping, D. Klostermeier, C. Herrmann, T. Veit, R. Seidel, J. Reinstein, Regulation of ATPase and chaperone cycle of DnaK from *Thermus thermophilus* by the nucleotide exchange factor GrpE, J. Mol. Biol. 305 (2001) 1173–1183.

[22] J.P. Grimshaw, I. Jelesarov, H.J. Schonfeld, P. Christen, Reversible thermal transition in GrpE, the nucleotide exchange factor of the DnaK heat-shock system, J. Biol. Chem. 276 (2001) 6098–6104.

Available online at www.sciencedirect.com
SCIENCE DIRECT®
Biochemical and Biophysical Research Communications 323 (2004) 339–344
BBRC
www.elsevier.com/locate/ybbrc

# Oligomeric Aip2p/Dld2p modifies the protein conformation of both properly folded and misfolded substrates in vitro

Naomi S. Hachiya[a,b,c], Yuji Sakasegawa[a,b], Hiroyuki Sasaki[d], Akiko Jozuka[a,b], Shoichiro Tsukita[b,e], Kiyotoshi Kaneko[a,c,*]

[a] *Department of Cortical Function Disorders, National Institute of Neuroscience, National Center of Neurology and Psychiatry, Tokyo 187-8502, Japan*
[b] *Tsukita Cell Axis Project, Exploratory Research for Advanced Technology (ERATO) and Solution Oriented Research for Science and Technology (SORST), Japan Science and Technology Corporation, Saitama 332-0012, Japan*
[c] *Core Research for Evolutional Science and Technology (CREST), Japan Science and Technology Agency, Saitama 332-0012, Japan*
[d] *Institute of DNA Medicine, The Jikei University School of Medicine, Tokyo 105-8461, Japan*
[e] *Department of Cell Biology, Faculty of Medicine, Kyoto University, Kyoto 606-8501, Japan*

Received 7 August 2004

**Abstract**

Oligomeric actin-interacting protein 2 (Aip2p) [Nat. Struct. Biol. 2 (1995) 28]/D-lactate dehydrogenase protein 2 (Dld2p) [Yeast 15 (1999) 1377, Biochem. Biophys. Res. Commun. 295 (2002) 910] exhibits the unique grapple-like structure with an ATP-dependent opening [Biochem. Biophys. Res. Commun. 320 (2004) 1271], which is required for the F-actin conformation modifying activity in vitro and in vivo [Biochem. Biophys. Res. Commun. 319 (2004) 78]. To further investigate the molecular nature of oligomeric Aip2p/Dld2p, the substrate specificity of its binding and protein conformation modifying activity was examined. In the presence of 1 mM ATP or AMP-PNP, oligomeric Aip2p/Dld2p bound to all substrates so far examined, and modified the conformation of actin, DNase I, the mature form of invertase, prepro-α-factor, pro-α-factor, and mitochondrial superoxide dismutase, as determined by the trypsin susceptibility assay. Of note, the activity could modify even the conformation of pathogenic highly aggregated polypeptides, such as recombinant prion protein in β-sheet form, α-synuclein, and amyloid β (1–42) in the presence of ATP. The in vivo protein conformation modifying activity, however, depends on the growth stage; the most significant substrate modification activity was observed in yeast cells at the log phase, suggesting the presence of a cofactor/s in yeast cells, where F-actin is supposed to be a major target in vivo. These data further support our previous notion that the oligomeric Aip2p/Dld2p may belong to an unusual class of molecular chaperones [Biochem. Biophys. Res. Commun. 320 (2004) 1271], which can target both properly folded and misfolded proteins in an ATP-dependent manner in vitro.


*Keywords:* Actin interacting protein 2; D-Lactate dehydrogenase protein 2; Oligomeric form; Trypsin susceptibility assay; ATP-dependent conformation modifying activity; Broad substrate specificity; β-Sheet conformation; Cell-cycle dependent

The actin and its interacting proteins play diverse roles in the cell, mediating endocytosis, exocytosis, cell motility, cell polarity, and cytokinesis [6]. Among them, a search for *Saccharomyces cerevisiae* proteins that interact with actin in the two-hybrid system identified the gene encoding Aip2p (YDL178w) [1], and the same gene product has been reported to exhibit D-lactate dehydrogenase (DLD) activity in vitro in yeast cells [2] as well as in mammalian cells [3].

We previously reported that the Aip2p [1]/Dld2p [2,3] exhibits an interaction with F-actin both in vitro and in vivo with its unique grapple-like structure and an ATP-dependent opening [5]. Incubation with Aip2p/Dld2p

* Corresponding author. Fax: +81 42 346 1748.
*E-mail address:* kaneko@ncnp.go.jp (K. Kaneko).

0006-291X/$ - see front matter © 2004 Elsevier Inc. All rights reserved.
doi:10.1016/j.bbrc.2004.08.098

facilitated the formation of the circular form of F-actin in vitro, which possessed an aberrant conformation compared to the linear form of F-actin. Overexpression of Aip2p induced multi-buds in yeast cells, whereas reduced expression interfered with the formation of the cleavage furrow for the cell division, which was rescued by the introduction of wild-type Aip2p. While Aip2p-treated F-actin in the circular form was negligibly stained by rhodamine-labeled phalloidin (rhodamine–phalloidin) in vitro, rhodamine–phalloidin staining profiles in actin interacting protein 2 gene (AIP2)-modified cells suggested a correlation between the conformation of F-actin and the expression of Aip2p in vivo. Furthermore, the AIP2-deleted cells became sensitive to an osmotic condition, which is a hallmark of actin dysfunction, and Aip2p/Dld2p co-immunoprecipitated with actin in yeast cells.

Following ultrastructural analysis revealed a novel oligomeric grapple-like structure of 10–12 subunits with an ATP-dependent opening [4]. ATP regulates the opening and closing of the "gate" that forms the opening within oligomeric Aip2p/Dld2p, where binding to the substrate occurs while in the open form. In the presence of ATP (open state), oligomeric Aip2p/Dld2p bound the F-actin fiber within the opening, whereas in the absence of ATP (closed state), no binding was observed. Simultaneously, the oligomeric Aip2p/Dld2p increased the trypsin susceptibility of F-actin in an ATP-dependent manner that ATP-binding rather than ATP hydrolysis is required for the protein conformation modifying reaction.

During our consecutive investigation, it was suggested that the oligomeric Aip2p/Dld2p also bound and modified the conformation of several protein substrates other than F-actin as determined by the trypsin susceptibility assay in vitro. Here, we further examined the substrate specificity of its binding property and protein conformation modifying activity. Of note, the oligomeric Aip2p/Dld2p could target both properly folded and even pathogenic highly aggregated proteins and thus, it exhibited no obvious substrate specificity for its binding and robust protein conformation modifying activity in vitro.

## Materials and methods

*Yeast strain and antibodies.* Protease deficient strain SH2777 was a gift from Dr. Harashima, Osaka University. Affinity-purified polyclonal rabbit anti-actin, anti-α-synuclein, and anti-heavy meromyosin (HMM) antibodies were purchased from Chemicon. Anti-cytochrome *c* antibody was purchased from BD Biosciences. Anti-SOD and anti-DNase I antibodies were purchased from Sigma Chemical. Affinity-purified polyclonal rabbit anti-invertase and anti-α-factor antibodies were raised against polypeptides harbouring 15 amino acid residues at the C-terminus, respectively. Anti-recombinant prion protein (PrP) antibody, K1, was rabbit polyclonal antibody raised against PrP residues 26–40 [7,8].

*Preparation of substrate proteins.* Amyloid β (1–28), amyloid β (1–42), cytochrome *c*, DNase I, malate dehydrogenase (MDH), and mitochondrial SOD were purchased from Sigma Chemical. α-Synuclein was purchased from Chemicon. HMM, luciferase, and the mature form of invertase were purchased from Wako Chemicals. Rabbit muscle actin was purchased from Molecular Probes. Two micromolar of rabbit muscle G-actin was polymerized in high salt buffer (10 mM Tris–Cl, pH 8.0, 100 mM KCl, and 2 mM $MgCl_2$) at 37 °C for 2 h, and used as F-actin. The gene fragments of hexahistidine-tagged ppαF and proαF were amplified by PCR, respectively, inserted into pET11a plasmid, expressed in *Escherichia coli* BL21(DE3) using the pET system, and purified according to the manufacturer's protocol (Qiagen, K.K.). Purified ppαF was dialyzed against buffer A (10 mM Hepes–KOH, pH 7.4, 1 mM DTT, and 1 mM $Mg(OAc)_2$) and subsequently used in the trypsin susceptibility protein conformation modifying assay. Recombinant PrP (rPrP) was purchased from Prionics, AG. The PrP solubilized in PBS was kept at 4 °C until circular dichroism detected over 50% of β-sheet contents in the rPrP, and then used as "PrP in β-sheet form."

*Surface plasmon resonance.* BIAcore 3000 system was used to analyze molecular interactions by means of surface plasmon resonance (SPR). Purified oligomeric form of Aip2p/Dld2p was covalently linked to a Sensor Chip CM5 (carboxymethylated dextran surface), with the use of amine coupling chemistry according to manufacturer's instructions. Samples for analyte proteins were diluted (10 μg $ml^{-1}$) in the running buffer (10 mM Hepes–KOH, pH 7.4, 150 mM NaCl, 1 mM $MgCl_2$, 3 mM EDTA, 0.005% surfactant P20, and 1 mM ATP), and injected over the surface at 4 °C with a flow rate of 5 μl $min^{-1}$. Each sensorgram was subtracted for the response observed in the control flow cell containing a blank surface and results were analyzed by using BIA evaluation SPR kinetic software (Biacore).

*Purification of hexahistidine-tagged Aip2p/Dld2p and trypsin susceptibility assay.* In an effort to obtain sufficient quantities of oligomeric Aip2p/Dld2p, the protein was prepared from the expression strain in yeast under control of the ADH promoter as previously described [4,5]. The trypsin susceptibility assay was performed as previously described [4,5,9–11]. Briefly, assays (200 μl) were initiated by adding 200 ng (if not indicated) of protein substrates to buffer B (10 mM Tris–Cl, pH 8.0, 0.1 M KCl, and 10 mM $MgCl_2$) containing 1 mM ATP and 500 ng of hexahistidine-tagged oligomeric Aip2p/Dld2p, and incubated at 30 °C for 15 min. After incubation, samples were treated with trypsin (0.2 μg $ml^{-1}$) at 16 °C for 15 min. The reaction was terminated by incubation with soybean trypsin inhibitor (0.4 μg $ml^{-1}$) on ice for 5 min, TCA-precipitated with tRNA carrier, and then subjected to SDS–PAGE and Western blotting with corresponding antibody at 1:1000 (unless otherwise noted). Immunoreactive bands were visualized by ECL-plus (Amersham Biosciences) and analyzed using a Fluoro SMAX (Bio-Rad).

## Results

### *Substrate recognition and binding of oligomeric Aip2p/Dld2p*

To examine the in vitro oligomeric Aip2p/Dld2p-substrate-binding specificity in detail, we performed a surface plasmon resonance (SPR) assay with a wide variety of proteins as binding substrates including amyloid β (1–28), amyloid β (1–42), α-synuclein, cytochrome *c*, F-actin, G-actin, HMM, Invertase, MDH, ppαF, proαF, PrP, and SOD. In the presence of 1 mM ATP (see Fig. 1A) or AMP-PNP (data not shown), oligomeric Aip2p/Dld2p bound to all substrates so far exam-

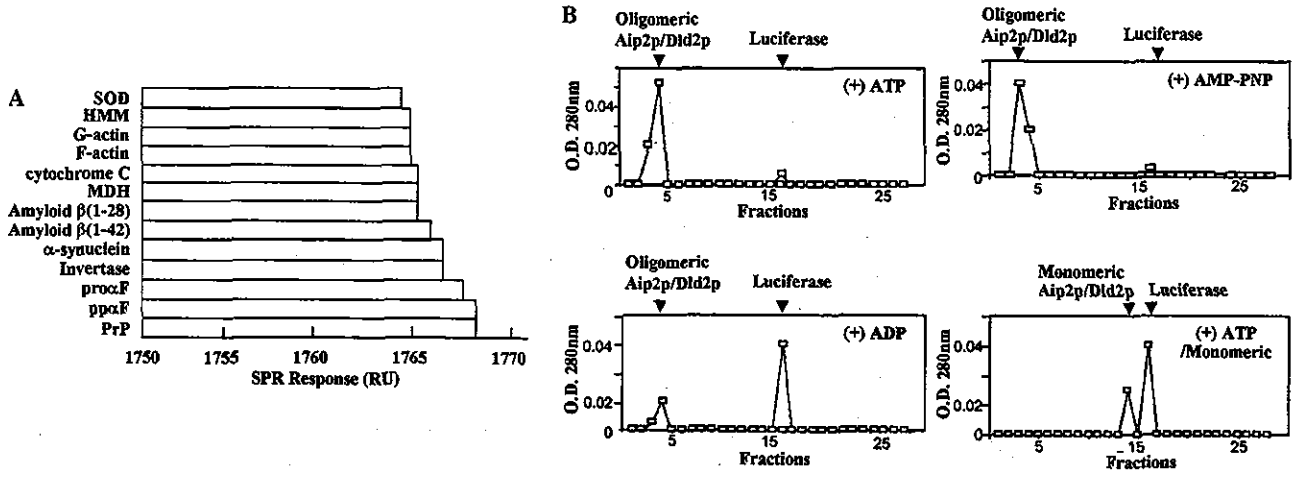


Fig. 1. Oligomeric Aip2p/Dld2p binds to all substrates examined in an ATP-dependent manner. (A) Interactions between oligomeric Aip2p/Dld2p and substrate proteins were measured by surface plasmon resonance (SPR) assay in the presence of ATP (see Materials and methods). SOD, superoxide dismutase; HMM, heavy meromyosin; MDH, malate dehydrogenase; proαF, pro-α-factor; ppαF, prepro-α-factor; and PrP, recombinant prion protein. (B) ATP requirement for its substrate-binding activity. Luciferase (300 ng) and oligomeric Aip2p/Dld2p (100 ng) were incubated in buffer B (see Materials and methods) with 1 mM ATP ((+) ATP), 1 mM AMP-PNP ((+) AMP-PNP), or 1 mM ADP ((+) ADP). Truncated monomeric Aip2p/Dld2p [4] could not bind substrate even in the presence of ATP ((+) ATP/monomeric). Each sample was passed through a gel filtration column (Superdex 200 column, Amersham BioSciences, Smart System).

ined, whereas oligomeric Aip2p/Dld2p bound to no substrates in the presence of ADP or with no nucleotides (data not shown). These data indicated that substrate-binding activity of oligomeric Aip2p/Dld2p requires ATP.

Gel filtration chromatography was then used to examine the oligomeric Aip2p/Dld2p–substrate interaction. Following incubation of luciferase with oligomeric Aip2p/Dld2p in the absence of ATP or presence of ADP, no oligomeric Aip2p/Dld2p–luciferase complex formation was observed, with both proteins being eluted separately (Fig. 1B, (+) ADP). In contrast, following incubation of both proteins in the presence of ATP or AMP-PNP, luciferase and oligomeric Aip2p/Dld2p eluted in fractions three and four as a complex (Fig. 1B, (+) ATP, and (+) AMP-PNP). Therefore, ATP and AMP-PNP induced the binding of oligomeric Aip2p/Dld2p to luciferase. This trend was also observed when ppαF and HMM were used as substrates (data not shown), indicating that substrate recognition is dependent on the binding of ATP to oligomeric Aip2p/Dld2p but not on ATP hydrolysis. In accordance with the result that the monomeric Aip2p/Dld2p with a C-terminal coiled-coil region-truncation failed to exhibit the conformation modifying activity [4], the coiled-coil region-truncated monomeric Aip2p/Dld2p exhibited no interaction with luciferase ((+) ATP/monomeric).

*Oligomeric Aip2p/Dld2p has no obvious substrate specificity for its robust ATP-dependent protein conformation modifying activity in vitro*

Oligomeric Aip2p/Dld2p increased the trypsin susceptibility of the substrate other than F-actin (ppαF, Fig. 2A, lanes 1, 2, and 4) in the presence of ATP. In the absence of ATP, however, the substrate was protected from trypsin digestion just as in the control (lanes 1 and 3), suggesting that this protein conformation modifying activity is ATP-dependent. Interestingly, further investigation revealed that the oligomeric Aip2p/Dld2p modified the conformation of actin, DNase I, the mature form of invertase, proαF, and mitochondrial SOD, as determined by the trypsin susceptibility assay (Fig. 2B). Thus, no obvious specific substrates have been identified for the protein conformation modifying activity of oligomeric Aip2p/Dld2p in vitro. Oligomeric Aip2p/Dld2p itself does not possess protease activity (Fig. 2C).

Use of the non-hydrolyzable ATP analog AMP-PNP yielded similar results to those observed with ATP, whereas the use of ADP failed to alter the luciferase activity (Fig. 2D), which is frequently used to analyze chaperone-mediated unfolding reactions as a properly folded protein substrate [12]. In accordance with our previous observation on the F-actin conformation modifying activity [4], these data further confirmed that ATP-binding rather than ATP hydrolysis is required for the protein conformation modifying reaction with other protein substrates, too.

In addition to the aforementioned indirect biochemical analyses suggesting that oligomeric Aip2p/Dld2p possesses protein conformation modifying activity, more direct evidence of this activity was sought through the use of low angle rotary shadowing [13]. Rabbit skeletal muscle HMM has a characteristic structure consisting of two globular heads and one tail (Fig. 3A, HMM). Following incubation with oligomeric Aip2p/Dld2p in the presence of 1 mM ATP, HMM heads were "unfold-

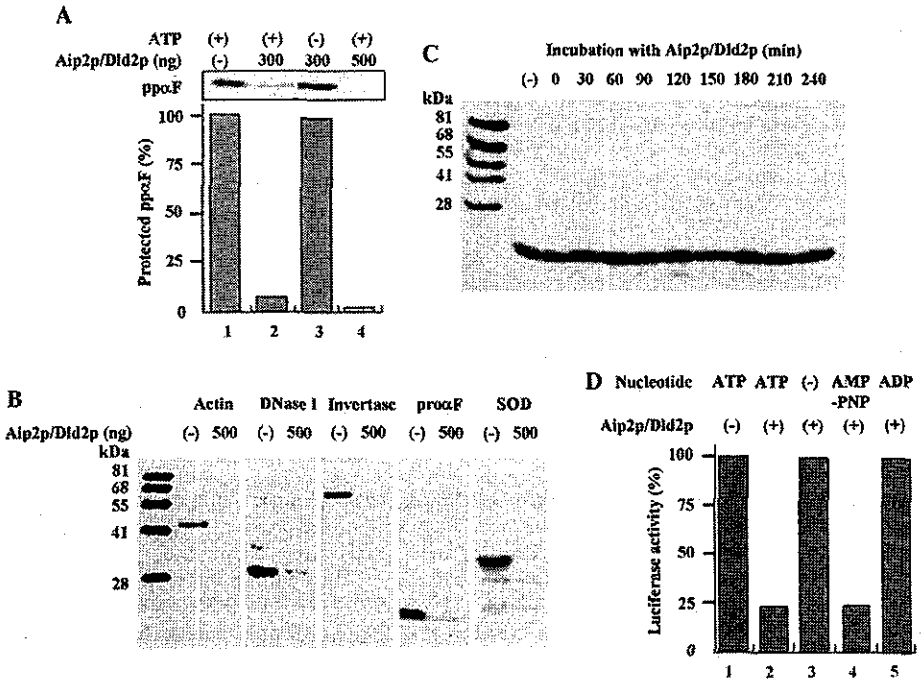


Fig. 2. Oligomeric Aip2p/Dld2p modifies the conformation of properly folded substrates in an ATP-dependent manner in vitro. (A) In the presence of ATP, Aip2p/Dld2p increases the protease susceptibility of ppαF (lanes 2 and 4). In the absence of ATP, no activity is observed (lane 3) and ppαF is resistant to trypsin digestion just as in the control (lane 1). (B) Trypsin susceptibility assay was further performed with protein substrates including actin (molecular weight = 41.8 kDa), DNase I (30 kDa), the mature form of recombinant invertase (60.6 kDa), proαF (13 kDa), and mitochondrial SOD (32.5 kDa). (C) Oligomeric Aip2p/Dld2p itself does not possess protease activity. Two hundred nanogram of ppαF was incubated with 500 ng of oligomeric Aip2p/Dld2p in the presence of 1 mM ATP for 0–240 min at 30 °C, and the signals were examined by Western blotting with anti-α-factor antibody. (D) The protein conformation modifying activity depends on ATP-binding. The firefly luciferase (300 ng) and oligomeric Aip2p/Dld2p (300 ng) were pre-incubated (final volume of 200 μl) with 1 mM ATP (lane 2), 1 mM ATP with excess amounts (10 mM) of AMP-PNP (lane 4), 1 mM ADP (lane 5) or without nucleotide (lane 3) in buffer A (see Materials and methods) for 15 min at 30 °C. The activity was assayed using the PicaGene luciferase assay kit (Wako Pure Chemicals) in a final volume of 1.2 ml, and the luciferin emission was determined using a luminometer (Stratec Biomedical Systems).

ed" and adopted an extended globular structure, while the helical tail became longer and thinner (Fig. 3A, Aip2p/Dld2p-HMM). Trypsin susceptibility of HMM also increased after the incubation with oligomeric Aip2p/Dld2p (Fig. 3A).

Surprisingly, even when pathogenic polypeptides such as the rPrP in β-sheet form, α-synuclein or amyloid β (1–42) peptide were tested as substrates in the trypsin susceptibility assay, it was found that trypsin susceptibility increased in the presence of oligomeric Aip2p/Dld2p. Although these pathogenic highly aggregated polypeptides (Fig. 3B) were resistant to 2.5 μg $ml^{-1}$ trypsin, digestion was significant in the presence of only 200 ng $ml^{-1}$ trypsin following incubation with oligomeric Aip2p/Dld2p (Fig. 3B).

*Protein conformation modifying activity depends on the growth stage*

In order to compare the protein conformation modifying activity in different cell cycles, hexahistidine-tagged oligomeric Aip2p/Dld2p was partially purified from synchronized cells during both log and stationary phases using Ni–NTA–agarose chromatography. The hexahistidine-tagged oligomeric Aip2p/Dld2p was then assayed for its protein conformation modifying activity using F-actin as a substrate. The activity of oligomeric Aip2p/Dld2p purified from log phase cells was almost fivefold greater than that measured in stationary phase cells (Fig. 4). Western blots using anti-Aip2p/Dld2p revealed that Aip2p/Dld2p expression was approximately equivalent in these two phases (Fig. 4), suggesting that the protein conformation modifying activity of oligomeric Aip2p/Dld2p varies with the cell growth stage.

## Discussion

The oligomeric Aip2p/Dld2p targeted both properly folded and pathogenic highly aggregated proteins, and exhibited a robust protein conformation modifying activity in vitro. It disrupted the tertiary structure of a variety of properly and stably folded substrate proteins such as the native form of luciferase, actin, HMM, mitochondrial SOD, MDH, and DNase I, as determined in

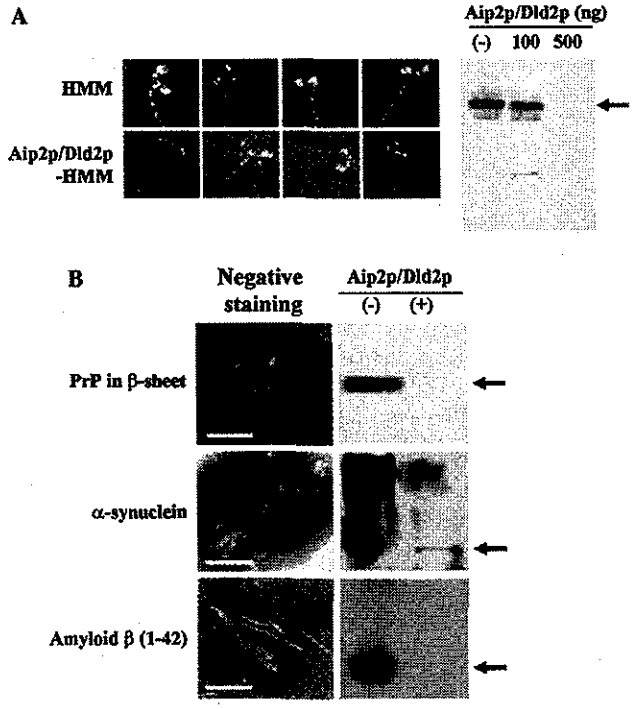


Fig. 3. Oligomeric Aip2p/Dld2p displays broad substrate specificity in vitro. (A) Heavy meromyosin (HMM) is unfolded by oligomeric Aip2p/Dld2p. One hundred microgram per milliliter of HMM was incubated with or without oligomeric Aip2p/Dld2p (100 μg $ml^{-1}$) in buffer A containing 1 mM ATP as described in Materials and methods. Following incubation, each mixture was subjected to low angle shadowing electron microscopy. Scale bar is 50 nm. Right panel represents the increased trypsin susceptibility of oligomeric Aip2p/Dld2p-treated HMM (100 and 500 ng). HMM was immunostained with anti-HMM polyclonal antibody. (B) Trypsin susceptibility of oligomeric Aip2p/Dld2p-treated pathogenic highly aggregated proteins is dramatically increased. Recombinant prion protein (PrP) in β-sheet form (20 μg), α-synuclein (20 μg), and amyloid β (1–42) peptide (60 μg) were used as specimens for negative staining (left panels). PrP in β-sheet form (300 ng), α-synuclein (200 ng) and amyloid β (1–42) peptide (400 ng) were used for the trypsin susceptibility assay (right panels). PrP and α-synuclein were immunostained with anti-PrP polyclonal antibody K1 (1:200) and anti-α-synuclein antibody, respectively. Amyloid β (1–42) peptide was silver stained according to the manufacturer's instruction (Wako Chemicals). Scale bars are 100 nm.

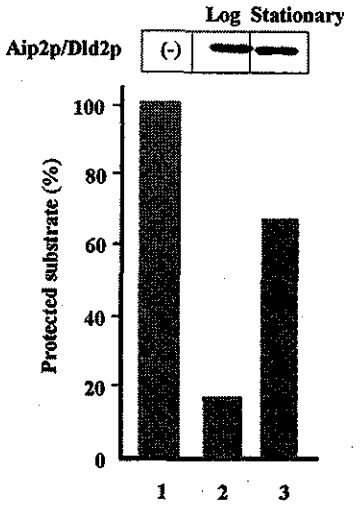


Fig. 4. Aip2p/Dld2p modifies the conformation of F-actin in vivo in a cell cycle-dependent manner. Analysis of protein conformation modifying activity of Aip2p/Dld2p in stationary and log phase yeast cells. Synchronized yeast cells constitutively expressing C-terminally hexahistidine-tagged Aip2p/Dld2p were grown to $OD_{600}$ of 0.5 (log phase, lane 2) or 11 (stationary phase, lane 3) and oligomeric Aip2p/Dld2p was purified from 10 mg each of total yeast cells according to the procedure described in Materials and methods. Protected actin band was detected according to the procedure of trypsin susceptibility assay. A thousandth of purified Aip2p/Dld2p at log or stationary phases was detected by Western blot analysis with anti-Aip2p/Dld2p antibody.

vitro. Both the substrate-binding and protein conformation modifying activities are regulated by the binding of ATP to Aip2p/Dld2p, but not by ATP hydrolysis.

This represents a distinct profile as reflected in known Group I and II chaperonins, which do not target the properly folded proteins [14–17]. In terms of the recognition of native (properly folded) proteins, the folding of native tubulin involves at least seven different chaperone proteins [18], while the structure of the yeast homolog of cofactor A, Rbl2p, is a dimer with largely hydrophilic surfaces, reflecting the fact that it interacts with quasi-native, and not unfolded, β-tubulin. In turn, these chaperone proteins do not recognize misfolded proteins. It is worth noting that the robust protein conformation modifying activity of oligomeric Aip2p/Dld2p modulated the conformation of several pathogenic, highly aggregated proteins such as PrP in β-sheet form associated with prion disease [19], α-synuclein associated with Parkinson's disease [20], and amyloid β (1–42) peptide associated with Alzheimer's disease [21].

As an example of the three-dimensional image of proteins with increased trypsin susceptibility, we directly visualized the "unfolded" structure of substrate protein (HMM) by oligomeric Aip2p/Dld2p with the low angle rotary shadowing electron microscopy. Based on our previous notion that the oligomeric Aip2p/Dld2p exhibits a grapple-like structure of 10–12 subunits with an ATP-dependent opening [4], we are tempted to speculate that substrate proteins probably enter the cavity of oligomeric Aip2p/Dld2p, where they were unfolded in the presence of ATP. Thus, protein unfolding seems to contribute, at least in part, to the aberrant trypsin susceptibility by oligomeric Aip2p/Dld2p.

When the oligomeric Aip2p/Dld2p regulates some protein metabolism in vivo through its unique protein conformation modifying activity, the activity as it is can be extremely dangerous for cells, as it exhibits broad substrate specificity in vitro. Thus, this activity has to be tightly controlled under very stringent regulation such as by other co-factor/s in vivo. In fact, partially purified Aip2p/Dld2p at the log phase possessed higher protein conformation modifying activity and ATP-binding capacity than that of Aip2p/Dld2p purified at the sta-

tionary phase, suggesting the presence of cofactor/s that may provide ATP to oligomeric Aip2p/Dld2p in yeast cells, where F-actin is supposed to be a major target in vivo [5].

Finally, these data further support our previous notion that the oligomeric Aip2p/Dld2p may belong to an unusual class of molecular chaperones [4]. The oligomeric Aip2p/Dld2p represents a unique grapple-like structure in an ATP-dependent opening, and is able to recognize both properly folded and highly aggregated proteins with broad substrate specificity in vitro. Whether these data represent a new regulatory mechanism of protein conformations in vivo has yet to be determined.

## Acknowledgments

We are indebted to G. Schatz, S.B. Prusiner, K. Mihara, and R.Scheckman for critical discussions and to I. Wada, N. Hoogenraad, M. Ryan, and A. Asano for helpful comments. We are also grateful to Y. Kozuka, K. Ihara, S. Yoshioka, M. Yamada, K. Watanabe, E.A. Nanri, and K. Ishibashi for technical assistance. This work was supported in part by grants from Exploratory Research for Advanced Technology (ERATO) and Core Research for Evolutional Science and Technology (CREST) of the Japan Science Technology Corporation (JST), Health and Labour Sciences Research Grants, Research on Advanced Medical Technology, nano-001, the Ministry of Health, Labour and Welfare of Japan, and the Naito Foundation.

## References

[1] D.C. Amberg, E. Basart, D. Botstein, Defining protein interactions with yeast actin in vivo, Nat. Struct. Biol. 2 (1995) 28–35.
[2] A. Chelstowska, Z. Liu, Y. Jia, D. Amberg, R.A. Butow, Signalling between mitochondria and the nucleus regulates the expression of a new D-lactate dehydrogenase activity in yeast, Yeast 15 (1999) 1377–1391.
[3] M.J. Flick, S.F. Konieczny, Identification of putative mammalian D-lactate dehydrogenase enzymes, Biochem. Biophys. Res. Commun. 295 (2002) 910–916.
[4] N.S. Hachiya, Y. Sakasegawa, S.H.A. Jozuka, S. Tsukita K. Kaneko, Oligomeric Aip2p/Dld2p forms a novel grapple-like structure and has an ATP-dependent F-actin conformation modifying activity in vitro, Biochem. Biophys. Res. Commun. 320 (2004) 1271–1276.
[5] N.S. Hachiya, Y. Sakasegawa, A. Jozuka, S. Tsukita, K. Kaneko, Interaction of D-lactate dehydrogenase protein 2 (Dld2p) with F-actin: implication for an alternative function of Dld2p, Biochem. Biophys. Res. Commun. 319 (2004) 78–82.
[6] T.D. Pollard, The cytoskeleton, cellular motility and the reductionist agenda, Nature 422 (2003) 741–745.
[7] N.S. Hachiya, K. Watanabe, Y. Sakasegawa, K. Kaneko, Microtubules-associated intracellular localization of the NH(2)-terminal cellular prion protein fragment, Biochem. Biophys. Res. Commun. 313 (2004) 818–823.
[8] N.S. Hachiya, K. Watanabe, M. Yamada, Y. Sakasegawa K. Kaneko, Anterograde and retrograde intracellular trafficking of fluorescent cellular prion protein, Biochem. Biophys. Res. Commun. 315 (2004) 802–807.
[9] N. Hachiya, R. Alam, Y. Sakasegawa, M. Sakaguchi, K. Mihara, T. Omura, A mitochondrial import factor purified from rat liver cytosol is an ATP-dependent conformational modulator for precursor proteins, EMBO J. 12 (1993) 1579–1586.
[10] N. Hachiya, T. Komiya, R. Alam, J. Iwahashi, M. Sakaguchi T. Omura, K. Mihara, MSF, a novel cytoplasmic chaperone which functions in precursor targeting to mitochondria, EMBO J. 13 (1994) 5146–5154.
[11] N. Hachiya, K. Mihara, K. Suda, M. Horst, G. Schatz T. Lithgow, Reconstitution of the initial steps of mitochondrial protein import, Nature 376 (1995) 705–709.
[12] E. Nimmesgern, F.U. Hartl, ATP-dependent protein refolding activity in reticulocyte lysate. Evidence for the participation of different chaperone components, FEBS Lett. 331 (1993) 25–30.
[13] S. Tsukita, Desmocalmin: a calmodulin-binding high molecular weight protein isolated from desmosomes, J. Cell Biol. 101 (1985) 2070–2080.
[14] T. Laufen, M.P. Mayer, C. Beisel, D. Klostermeier, A. Mogk J. Reinstein, B. Bukau, Mechanism of regulation of hsp70 chaperones by DnaJ cochaperones, Proc. Natl. Acad. Sci. USA 96 (1999) 5452–5457.
[15] R. Russell, A. Wali Karzai, A.F. Mehl, R. McMacken, DnaJ dramatically stimulates ATP hydrolysis by DnaK: insight into targeting of Hsp70 proteins to polypeptide substrates, Biochemistry 38 (1999) 4165–4176.
[16] Y. Groemping, D. Klostermeier, C. Herrmann, T. Veit, R. Seidel, J. Reinstein, Regulation of ATPase and chaperone cycle of DnaK from *Thermus thermophilus* by the nucleotide exchange factor GrpE, J. Mol. Biol. 305 (2001) 1173–1183.
[17] J.P. Grimshaw, I. Jelesarov, H.J. Schonfeld, P. Christen, Reversible thermal transition in GrpE, the nucleotide exchange factor of the DnaK heat-shock system, J. Biol. Chem. 276 (2001) 6098–6104.
[18] J. Martin, Group II chaperonins as mediators of cytosolic protein folding, Curr. Protein Pept. Sci. 1 (2000) 309–324.
[19] M.P. Mayer, H. Schroder, S. Rudiger, K. Paal, T. Laufen B. Bukau, Multistep mechanism of substrate-binding determines chaperone activity of Hsp70, Nat. Struct. Biol. 7 (2000) 586–593.
[20] J.T. Greenamyre, T.G. Hastings, Biomedicine. Parkinson's-divergent causes, convergent mechanisms, Science 304 (2004) 1120–1122.
[21] J.W. Lustbader, M. Cirilli, C. Lin, H.W. Xu, K. Takuma N. Wang, C. Caspersen, X. Chen, S. Pollak, M. Chaney F. Trinchese, S. Liu, F. Gunn-Moore, L.F. Lue, D.G. Walker, P. Kuppusamy, Z.L. Zewier, O. Arancio, D. Stern, S.S. Yan H. Wu, ABAD directly links a beta to mitochondrial toxicity in Alzheimer's disease, Science 304 (2004) 448–452.

Available online at www.sciencedirect.com
SCIENCE DIRECT®
Neuroscience Letters 374 (2005) 98–103
Neuroscience Letters
www.elsevier.com/locate/neulet

# Mitochondrial localization of cellular prion protein ($PrP^C$) invokes neuronal apoptosis in aged transgenic mice overexpressing $PrP^C$

Naomi S. Hachiya[a,b], Makiko Yamada[a,b], Kota Watanabe[a,b], Akiko Jozuka[a,b], Takuya Ohkubo[a,c], Kenichi Sano[a,1], Yoshio Takeuchi[a,2], Yoshimichi Kozuka[d], Yuji Sakasegawa[a], Kiyotoshi Kaneko[a,b,*]

[a] *Departments of a Cortical Function Disorders, National Institute of Neuroscience (NIN), National Center of Neurology and Psychiatry (NCNP), Kodaira, Tokyo 187-8502, Japan*
[b] *Core Research for Evolutional Science and Technology (CREST), Japan Science and Technology Agency, Kawaguchi, Saitama 332-0012, Japan*
[c] *Department of Neurology and Neurological Science, Graduate School of Medicine, Tokyo Medical and Dental University, Bunkyo-ku, Tokyo 113-0034, Japan*
[d] *Ultrastructural Research, National Institute of Neuroscience (NIN), National Center of Neurology and Psychiatry (NCNP), Kodaira, Tokyo 187-8502, Japan*

Received 14 September 2004; received in revised form 12 October 2004; accepted 13 October 2004

**Abstract**

Recent studies suggest that the disease isoform of prion protein ($PrP^{Sc}$) is non-neurotoxic in the absence of cellular isoform of prion protein ($PrP^C$), indicating that $PrP^C$ may participate directly in the neurodegenerative damage by itself. Meanwhile, transgenic mice harboring a high-copy-number of wild-type mouse (Mo) $PrP^C$ develop a spontaneous neurological dysfunction in an age-dependent manner, even without inoculation of $PrP^{Sc}$ and thus, investigations of these aged transgenic mice may lead to the understanding how $PrP^C$ participate in the neurotoxic property of PrP. Here we demonstrate mitochondria-mediated neuronal apoptosis in aged transgenic mice overexpressing wild-type $MoPrP^C$ (Tg(MoPrP)4053/FVB). The aged mice exhibited an aberrant mitochondrial localization of $PrP^C$ concomitant with decreased proteasomal activity, while younger littermates did not. Such aberrant mitochondrial localization was accompanied by decreased mitochondrial manganese superoxide dismutase (Mn-SOD) activity, cytochrome *c* release into the cytosol, caspase-3 activation, and DNA fragmentation, most predominantly in hippocampal neuronal cells. Following cell culture studies confirmed that decrease in the proteasomal activity is fundamental for the $PrP^C$-related, mitochondria-mediated apoptosis. Hence, the neurotoxic property of $PrP^C$ could be explained by the mitochondria-mediated neuronal apoptosis, at least in part.


*Keywords:* $PrP^C$; Proteasomal activity; Mitochondrial localization; Superoxide dismutase activity; Mitochondria-mediated apoptosis

The posttranslational conformational change of the cellular isoform of prion protein ($PrP^C$) into its scrapie isoform ($PrP^{Sc}$) is the fundamental process underlying the pathogenesis of prion diseases [24], but the molecular events through which prion infection and the resulting accumulation of PrP lead to the neuronal dysfunction, vacuolation, and death that characterize prion pathology remain unclear [6].

Importantly, $PrP^{Sc}$, the disease isoform of PrP, seems to be non-neurotoxic in the absence of $PrP^C$, suggesting that $PrP^C$ may participate directly in the prion neurodegenerative damage by itself, and the cellular pathways activated by neurotoxic forms of PrP that ultimately result in neuronal death are also being investigated, and several possible mechanisms have been uncovered [6]. For example, cross-linking

* Corresponding author. Tel.: +81 42 346 1718; fax: +81 42 346 1748.
*E-mail address:* kaneko@ncnp.go.jp (K. Kaneko).
[1] Present address: Hinoieda Kagaku Ltd., Hino-city, Tokyo 191-0061, Japan.
[2] Present address: KOHJIN-BIO Ltd., Sakado-city, Saitama 350-0214, Japan.

0304-3940/$ – see front matter © 2004 Elsevier Ireland Ltd. All rights reserved.
doi:10.1016/j.neulet.2004.10.044

$PrP^C$ in vivo with specific monoclonal antibodies was found to trigger neuronal apoptosis, suggesting that $PrP^C$ functions in the control of neuronal survival [26]. In fact, neural tissues overexpressing $PrP^C$ grafted into the brains of $PrP^C$-deficient mice develop the severe histopathological changes characteristic of prion disease when infected with prions, but no pathological changes were seen in $PrP^C$-deficient tissue, not even in the immediate vicinity of the grafts despite the presence of high levels of $PrP^{Sc}$ [2]. In addition, interruption of $PrP^C$ expression during an ongoing prion infection prevents neuronal loss and reverses early spongiform change [16]. The continued accumulation of $PrP^{Sc}$ in this model after neuronal $PrP^C$ depletion is likely to reflect prion replication predominantly in both microglia and astrocytes glial cells without $PrP^C$ depletion, which support $PrP^{Sc}$ replication. The $PrP^{Sc}$ deposits colocalize with astrocytes in the brains of infected mice with neuronal $PrP^C$ depletion, which was not seen in scrapie-infected control animals without PrP depletion. The fact that these mice remain asymptomatic indicates that even extensive extraneuronal $PrP^{Sc}$ replication does not cause clinical disease or neurodegeneration in this model. Thus, neuronal $PrP^C$ seems to be fundamental for the neurotoxic property of PrP even in the $PrP^{Sc}$-infected conditions, but the detailed molecular events especially with non-mutant, wild-type $PrP^C$ still remained unclear.

Meanwhile, aged transgenic mice harboring a high-copy-number of wild-type PrP-B transgenes spontaneously developed mitochondrial encephalomyopathy including focal vacuolation of the central nervous system, skeletal muscles and peripheral nerves without $PrP^{Sc}$ inoculation [28]. Such focal vacuolation was localized to the hippocampus, the superior colliculus, and midbrain tegmentum, which resembled that seen in experimental scrapie, albeit less intense. Other transgenic lines harboring a high-copy-number of wild-type PrP transgenes also exhibited spontaneous neurological dysfunction in an age-dependent manner [21,27]. For example, transgenic mice overexpressing the wild-type mouse (Mo) *PrP-A gene* (Tg(MoPrP)4053/FVB) used in this study became symptomatic at around the age of 700 days, although no pathological evidence for prion diseases was evident [27]. Since no $PrP^{Sc}$ has been inoculated in these mice, investigations of these aged transgenic mice overexpressing wild-type $PrP^C$ may lead to the better understanding how $PrP^C$ participate in the neurotoxic property of PrP.

Here we show that the Tg(MoPrP)4053/FVB mice exhibited an aberrant mitochondrial localization of $PrP^C$ accompanied by decreased mitochondrial manganese superoxide dismutase (Mn-SOD) activity, cytochrome *c* release in the cytosol, caspase-3 activation, and DNA fragmentation, concomitant with decreased proteasomal activity in an age-dependent manner.

Tg(MoPrP)4053/FVB and its littermate were kindly provided by Dr. S.B. Prusiner (University of California, San Francisco). Antibodies K3 and K4 against PrP were rabbit polyclonal sera raised against PrP peptides corresponding to residues 76–90 and 96–110 in MoPrP, respectively. Anti-cytochrome *c* and anti-porin antibodies were purchased from BD Biosciences. Anti-Hsc70 antibody was purchased from Stressgen Biotechnologies Corporation. Mitotracker Red CMXRos was purchased from Molecular Probes. Lactacystin, ALLN, and MG132 were purchased from Sigma. The $\Delta\Psi m$ detection kit and APO-BrdU TUNEL assay kit were purchased from Trevigen Inc. and Molecular Probes, respectively. Antibodies were used at 1:1000 (Western blotting) or 1:100 (immunofluorescence microscopy) unless otherwise noted. For immuno-electronmicroscopy, 10 nm golds were purchased from DAKO.

Cells or brains were homogenized with 9 volumes of mitochondrial buffer (220 mM mannitol, 70 mM sucrose, 10 mM Hepes-KOH, pH 7.4, and 0.1 mM EDTA) and centrifuged at $700 \times g$ for 5 min at 4 °C, and the supernatant was further centrifuged at $5000 \times g$ for 10 min at 4 °C. The supernatant was used as a post-mitochondrial supernatant. The resulted pellet was washed three times with mitochondrial buffer, resuspended in 9 volumes of the same buffer, and then centrifuged at $2000 \times g$ for 2 min at 4 °C followed by $5000 \times g$ for 8 min at 4 °C. The pellet was resuspended in 9 volumes of the same buffer, and then centrifuged at $5000 \times g$ for 10 min at 4 °C. The final pellet was recovered and stored on ice until use (mitochondrial fraction). The post-mitochondrial supernatant was further centrifuged at $100{,}000 \times g$ for 1 h at 4 °C, and the supernatant was used as cytosolic fraction, and the pellet was resuspended in mitochondrial buffer (microsome fraction). Western blots were performed at 5 μg of total protein/lane.

Mitochondrial manganese superoxide dismutase (Mn-SOD) and cytosolic copper/zinc SOD (Cu/Zinc-SOD) activities were measured by the SOD assay kit (Dojindo Molecular Technologies, Inc.), and cytosolic glutathione (GSH) was measured by the Glutathione quantification kit (Dojindo Molecular Technologies, Inc.) according to the manufacturer's instructions. Caspase-3 activity was measured using the PARP Western Blot Kit (WAKO) according to the manufacturer's instructions. DNA fragmentation was measured by the TUNEL assay (ApopTag® Peroxidase *In situ* Apoptosis Detection Kit, CHEMICON International), which was performed according to the manufacturer's instructions before being visualized with an Olympus CX40 (Olympus Optical Co., Ltd.). Sections were counter-stained by 0.5% methyl green (WAKO) in 0.1 M sodium acetate (pH 4.0).

Proteasomal activity assay was performed as previously described [3,9,31].

Tg(MoPrP)4053/FVB harboring a high-copy-number of wild-type PrP-A transgenes at the age of 520 days (TG520) and an age-matched non-transgenic littermate (WT520) showed similar migration rates of $PrP^C$ on poly acrylamide gel electrophoresis and Western blotting using anti-PrP-antibody K4 (Fig. 1A, PK(−)). As increased resistance to protease K digestion is often a feature of $PrP^{Sc}$, this was examined in TG520 and WT520. No resistance to proteinase K digestion was detected in any of these mice (Fig. 1A, PK(+)). Histological examinations of the TG520 brains including

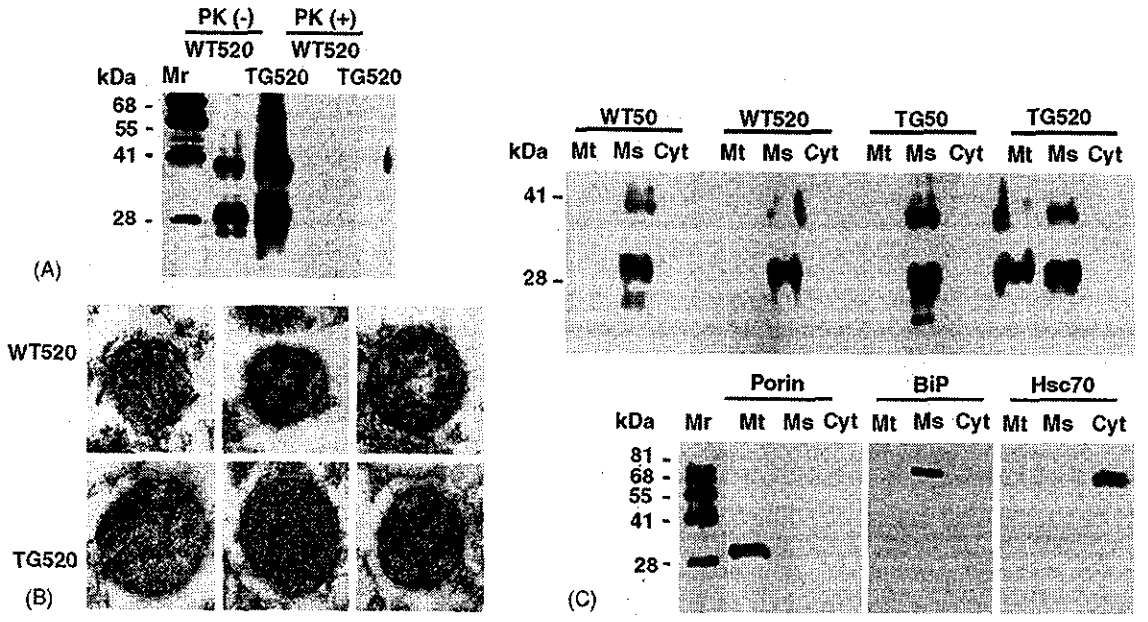


Fig. 1. $PrP^C$ is localized to the mitochondrial fraction in Tg(MoPrP)4053/FVB overexpressing wild-type $PrP^C$. WT520: non-transgenic littermate at the age of 520 days. TG520: Tg(MoPrP)4053/FVB at the age of 520 days. WT50: non-transgenic littermate at the age of 50 days. TG50: Tg(MoPrP)4053/FVB at the age of 50 days. (A) Western blot analysis and resistance to proteinase K digestion of $PrP^C$ in WT520 and TG520. PK(−): Western blot analysis with anti-PrP antibody K4. Bands derived from $PrP^C$ appear to be normal. PK(+): resistance to proteinase K digestion. Five hundred microliter of brain homogenates (5 μg of total protein/lane) were digested with proteinase K (20 μg/ml, Sigma) at 37 °C for 1 h followed by centrifugation at 100,000 × *g* for 1 h at 4 °C and the resuspended pellet was loaded onto the gels. No resistance to proteinase K digestion is detected. Mr: molecular weight marker. (B) Immuno electron microscopy (30,000×) detects $PrP^C$ with anti-PrP K3 (10 nm golds) in the mitochondria of neuronal cells in TG520. (C) Total brain homogenates of TG520 exhibit aberrant localization of overexpressed $PrP^C$, whereas those of WT50, WT520 and TG50 do not. Western blot analysis with anti-PrP antibody K4 (1:1000). Anti-porin antibody (1:1000) was used as a mitochondrial (Mt) marker, anti-BiP antibody (1:1000) was used as a microsome (Ms) marker, and anti-Hsc70 antibody (1:1000) was used as a cytosolic (Cyt) marker.

dentate gyrus, hippocampus, other cerebral cortices, basal ganglia and cerebellum by hematoxylin and eosin as well as methyl green-pyronin staining revealed no apparent pathological evidence in the brain sections of WT520 and TG520 (data not shown).

Since older transgenic mice (not inoculated with $PrP^{Sc}$) that harbor a high-copy-number of wild-type PrP-B transgenes develop mitochondrial encephalomyopathy including focal vacuolation of the central nervous system, skeletal muscles and peripheral nerves [28], we set out to determine whether $PrP^C$ could be detected in the mitochondrial fraction of TG520. Although the TG520 appeared clinically and histologically normal, they exhibited aberrant mitochondrial localization of $PrP^C$ as determined by immuno electron microscopy; immunogold-labelled $PrP^C$ localized at the mitochondria of the granular cells in the hippocampal dentate gyrus of TG520 but not of WT520 (Fig. 1B). Such aberrant mitochondrial localization of $PrP^C$ was further confirmed in TG520 by Western blotting using a subcellular fractionation, whereas younger non-transgenic littermate at the age of 50 days (WT50), WT520, and younger Tg(MoPrP)4053/FVB at the age of 50 days (TG50) did not exhibit the feature (Fig. 1C).

The oxidative stress leads to dysfunctions of the respiratory enzymes and the depletion of ATP followed by a decrease in reduced glutathione (GSH) concentration, which triggers the cycle of oxidative stress, mitochondrial dysfunction, and further antioxidant depletion. Exposure of tissue to oxygen free radicals results in lipid peroxidation, protein oxidation and DNA damage, which is in concert with "apoptosis". In order to prevent such damages, mammalian cells are equipped with both non-enzymatic and enzymatic scavenging systems to eliminate oxygen free radicals, anti oxidant enzymes, i.e., SOD, catalase, and glutathione peroxidase are essential to cells in removing $O_2^-$ and hydrogen peroxide ($H_2O_2$) from the tissues exposed to oxidative stress. Therefore, we next examined mitochondrial Mn-SOD as well as cytosolic Cu/Zn-SOD activities.

The mitochondrial Mn-SOD activity decreased significantly in TG520 compared to that in WT50, TG50, or WT520 (Fig. 2A), whereas no significant difference in the cytosolic copper/zinc SOD (Cu/Zn-SOD) activity was observed among them (Fig. 2B). Furthermore, cytosolic GSH level was dramatically decreased in TG520 but not in WT50, TG50, or WT520 (Fig. 2C). These results indicated that mitochondria-localized $PrP^C$ induced oxidative stress in TG520.

Subsequently, release of cytochrome *c* from the inner-membrane space into the cytosol (Fig. 3A), caspase-3 activation (Fig. 3B), and DNA fragmentation (Fig. 3C) were observed in TG520 brain, whereas no release of cytochrome *c*/ DNA fragmentation but faint caspase-3 activation was detected in WT520 brain (Fig. 3A–C). Serial specimens of TG520 and WT520 brains were further examined by

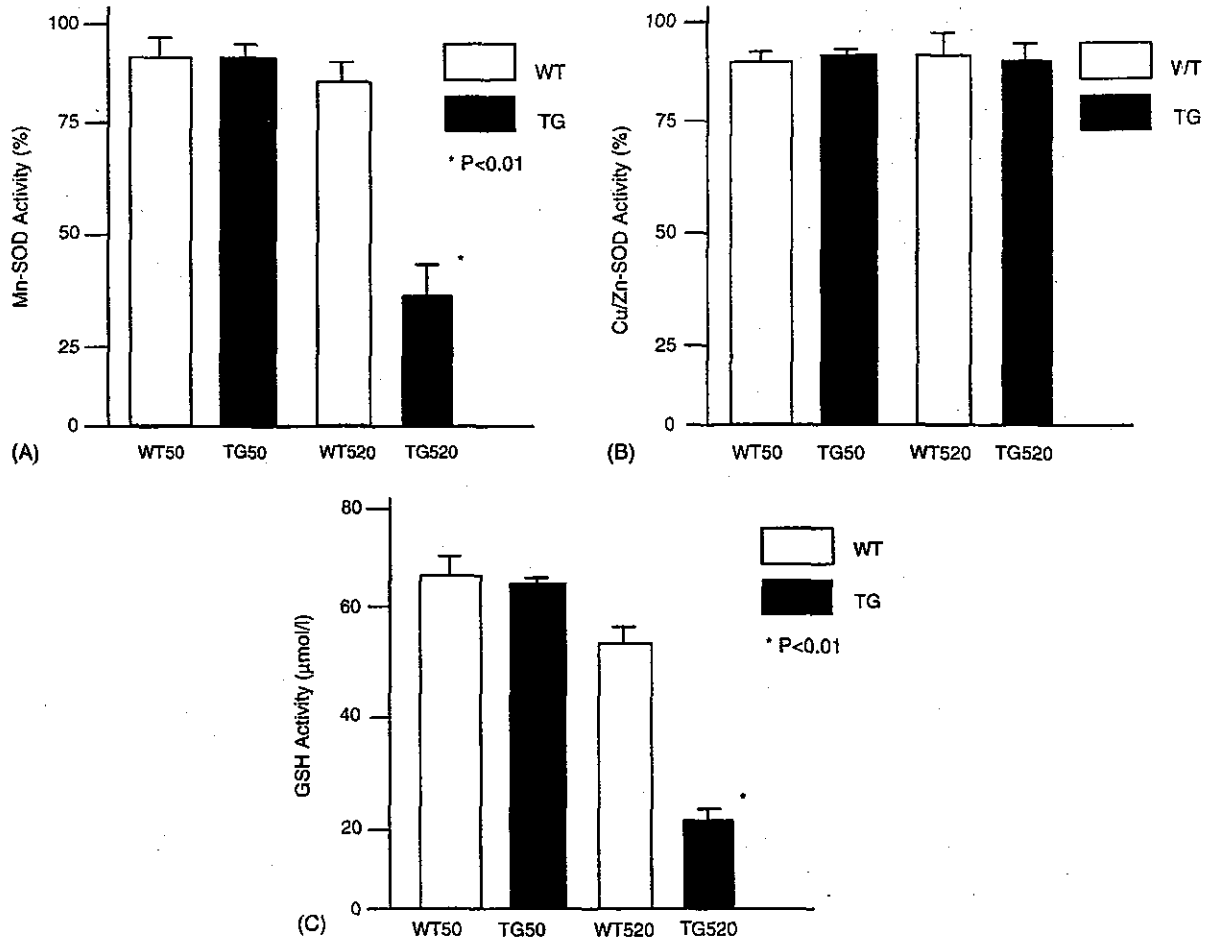


Fig. 2. Mitochondria-localized $PrP^C$ induces oxidative stress in TG520. (A) Mitochondrial manganese superoxide dismutase (Mn-SOD) and (B) cytosolic copper/zinc SOD (Cu/Zinc-SOD) activities. The Mn-SOD activity decreases significantly in TG520 compared to that in WT50, TG50 or WT520, whereas the cytosolic Cu/Zn-SOD activity remained similar among them. Error bars represent mean ± S.D. (C) Cytosolic glutathione (GSH) level is dramatically decreased in TG520 but not in WT50, TG50, or WT520. Error bars represent mean ± S.D.

the TUNEL assay (Fig. 3D). As shown, the TUNEL assay showed that the DNA fragmentation most predominantly in granular cells in the hippocampal dentate gyrus and to a lesser extent pyramidal cells in the CA1 and CA2 regions of TG520 (Fig. 3D).

In an age-dependent development of other aggregation disorders, the accumulation and aggregation of the disease related-proteins are associated with an age-dependent decrease in proteasomal activity and are promoted by inhibition of proteasomal activity [31]. Therefore, it is also likely that such aberrant mitochondrial localization requires $PrP^C$ retained in the cytoplasm with the proteasomal activity decreased. Therefore, the hydrolysis of Suc-Leu-Leu-Val-Tyr-4-methyl-coumaryl-7-amide (Suc-LLVY-MCA) by chymotrypsin-like proteasomal activity in brain homogenates of WT50, WT520, TG50, and TG520 was then investigated. As expected, proteasomal activity of both transgenic mice Tg(MoPrP)4053/FVB and non-transgenic littermate decreased with increasing age (Fig. 3E).

The posttranslational conformational change of $PrP^C$ into $PrP^{Sc}$ is the fundamental process underlying the pathogenesis of prion diseases [24]. Many concurrent reports have suggested that $PrP^C$ may play a role in neuronal survival or death. The removal of serum from cells in culture causes apoptosis in $PrP^C$-deleted cells but not in wild-type cells [13]. $PrP^C$ also inhibits Bax-mediated neuronal apoptosis in human primary neurons [1]. The binding of a ligand to $PrP^C$ transduces neuroprotective signaling through a cAMP/PKA-dependent pathway. Therefore, $PrP^C$ may function as a trophic receptor whose activation results in a neuroprotective state [5].

On the other hand, misfolded $PrP^C$ is subject to degradation by proteasomes. Like many misfolded secretory proteins [12,23], it is recognized in the ER and subject to retrograde transport to the cytoplasm and degradation by the proteasome [11,14,29,30]. Or, a small fraction of PrP chains is not translocated into the ER lumen during synthesis, and is rapidly degraded in the cytoplasm by the proteasome as far as proteasome function remains normal [8]. As proteasome function gradually decreases with age over a very long period or with inhibitors in the case of cultured cells, $PrP^C$ overflows in the cytoplasm, targeted to the mitochondria, which subsequently induces the mitochondria-mediated apoptosis.

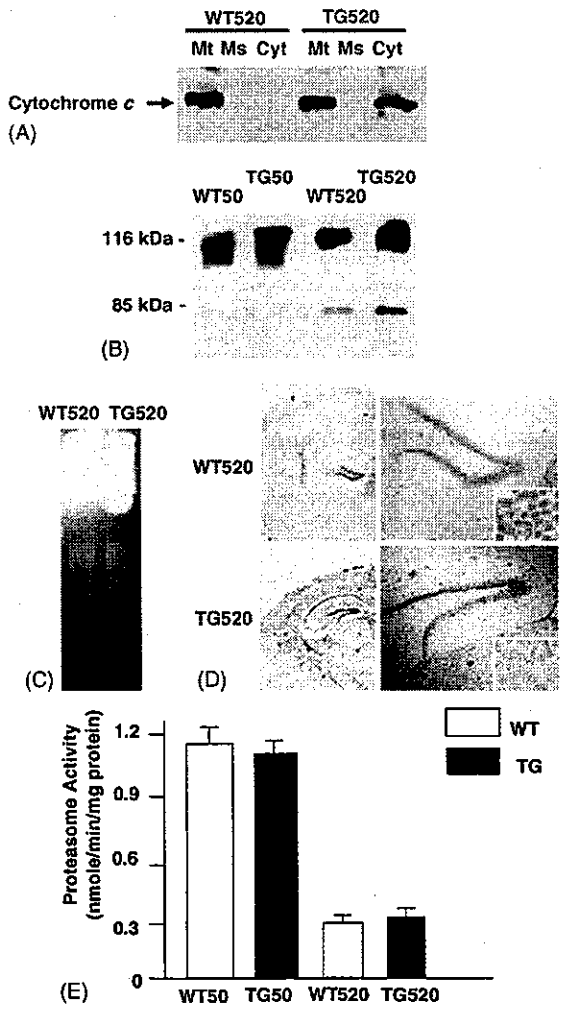


Fig. 3. Neuronal apoptosis in the TG520 brain. (A) Measurement of cytochrome *c* released into the cytosol. Western blot analysis with anti-cytochrome *c* antibody detects cytochrome *c* in the cytosol of the TG520 but not WT520 brain. Mt: mitochondrial fraction, Ms: microsome fraction, Cyt: cytosolic fraction. (B) Caspase-3 activation in TG520 brain. Brain homogenates (5 μg of total protein/lane) of younger WT50 and TG50 do not exhibit caspase-3 activation. Note that a faint band is detected in WT520 brain. The 85 kDa bands corresponding to the degradation products of poly ADP-ribose polymerase (PARP, 116 kDa) is a measure of caspase-3 activity. (C) DNA fragmentation in brain homogenates of TG520 is shown (1 μg of genomic DNA/lane). Brain homogenates of WT520 show no DNA fragmentation. Genomic DNAs were applied onto 1% agarose gel. (D) Serial frozen sections of total brains (left panels) and the hippocampal regions (right panels, 40×, lower right corner panels, 400×) were made. Top panels: WT520. Bottom panels: TG520. Neuronal apoptosis (brown) is evident in the bottom panels as compared with the top panels. (E) Age-dependent decrease in brain proteasomal activity. Chymotrypsin-like proteolytic activity was assayed in brain homogenates (1 μg of total protein/assay) of WT50, TG50, WT520, and TG520. Error bars represent mean ± S.D. ($n = 3$).

In fact, accumulation of $PrP^C$ in the cytoplasm is known to be strongly neurotoxic in both transgenic mice overexpressing the cytosolic form of $PrP^C$ [15] and cyclosporin A-treated cultured cells [7]. In these systems, $PrP^C$ expression enhances staurosporine-stimulated neuronal toxicity and DNA fragmentation, caspase-3-like activity and p53 transcriptional activities, all of which suggests that $PrP^C$ sensitizes neurons to apoptotic stimuli through caspase-3-mediated activation [20]. Proteasome inhibitors increase $PrP^C$-like immunoreactivity and unmask basal caspase-3 activation [19].

Despite these efforts, little is known about the $PrP^C$ localization and its metabolic fate in the cytoplasm. Ma et al. reported that PrP accumulated in the cytoplasm when proteasomal activity was compromised, and $PrP^C$ formed aggregates, often in association with Hsc70 [14]. With prolonged incubation, these aggregates accumulate in an "aggresome"-like state, surrounding the centrosome. Contrary to this report, other investigators reported there was a prominent shift in the intracellular locations of PrP immunostaining, but there was no "aggresome"-like PrP accumulation in the centrosome region [29]. The PrP signal was especially pronounced around the nucleus, and this signal only partially overlapped with both ER (calnexin, BiP and concanavalin A) and Golgi (wheat germ agglutinin). Thus, further examination has been awaited for determining the precise intracellular localization of $PrP^C$ in the cytoplasmic face.

With an artificial PrP peptide corresponding to PrP residues 106–126 [PrP(106–126)], chronic exposure of primary rat hippocampal cultures to micromolar concentrations of the peptide induces neuronal death with DNA fragmentation in degenerating neurons, having indicated apoptotic cell death [10]. The earliest detectable apoptotic event was the rapid depolarization of mitochondrial membranes, occurring immediately following treatment of cells with PrP(106–126). Subsequently, cytochrome *c* was released and caspase-3 was activated. It has also been demonstrated that the fusogenic peptide PrP(118–135) induced time- and dose-dependent apoptosis in rat cortical and retinal neurons that included caspase-3 activation and DNA condensation/fragmentation [4,22]. These results have implicated mitochondria as the primary site of action [18]. Unfortunately, this implication has been restricted to the cell death with the artificial PrP peptides, and thereby further illustrates the significance of our current observations in terms of the neurotoxic property of wild-type $PrP^C$ in vitro and in vivo.

There are potentially other mechanisms involved in neurotoxicity of the $PrP^{Sc}$-infected conditions, for example astrocytes, microglial cells and cytokines [17,25]. The activation of glial cells, which precedes neuronal death, and subsequent release of cytokines/chemokines may also contribute directly or indirectly to the neuronal cell death in prion diseases. In mutant $PrP^C$ metabolism, on the other hand, the ER also seems to play another important role as well. Mutant PrP(Q217R) remains associated with the chaperone BiP at the ER for an abnormally long period of time and is degraded by the proteasomal pathway [11]. Nonetheless, our current observations suggest that wild-type $PrP^C$ participate in the prion neurodegenerative cascade through the mitochondria-mediated events, at least in part. At the same time, the segregation of the infectious and neurotoxic properties of PrP suggests a new therapeutic strategy since prevention of mitochondrial mislocalization of $PrP^C$ can be regarded as putative therapeutic targets aimed at protecting

cells from mitochondria-mediated apoptosis, even though the prion infection is not fully preventable.

## Acknowledgements

We thank S.B. Prusiner for providing Tg(MoPrP)4053/FVB, T. Onodera for providing HpL3-4 cells, E. Nannri, K. Ishibashi, C. Ota, Y. Yamaura, and S. Wajima for technical assistance. We are indebted to G. Schatz, T. Omura, K. Mihara, R. Scheckman, and T. Momoi for helpful comments. This work was supported by grants from the Core Research for Evolutional Science and Technology (CREST) of the Japan Science and Technology Agency, Health and Labour Sciences Research Grants, Research on Advanced Medical Technology, nano-001, and the Ministry of Health, Labor and Welfare of Japan.

## References

[1] Y. Bounhar, Y. Zhang, C.G. Goodyer, A. LeBlanc, Prion protein protects human neurons against Bax-mediated apoptosis, J. Biol. Chem. 276 (2001) 39145–39149.
[2] S. Brandner, S. Isenmann, A. Raeber, M. Fischer, A. Sailer, Y. Kobayashi, S. Marino, C. Weissmann, A. Aguzzi, Normal host prion protein necessary for scrapie-induced neurotoxicity, Nature 379 (1996) 339–343.
[3] N. Canu, C. Barbato, M.T. Ciotti, A. Serafino, L. Dus, P. Calissano, Proteasome involvement and accumulation of ubiquitinated proteins in cerebellar granule neurons undergoing apoptosis, J. Neurosci. 20 (2000) 589–599.
[4] J. Chabry, C. Ratsimanohatra, I. Sponne, P.P. Elena, J.P. Vincent, T. Pillot, In vivo and in vitro neurotoxicity of the human prion protein (PrP) fragment P118–135 independently of PrP expression, J. Neurosci. 23 (2003) 462–469.
[5] L.B. Chiarini, A.R. Freitas, S.M. Zanata, R.R. Brentani, V.R. Martins, R. Linden, Cellular prion protein transduces neuroprotective signals, EMBO J. 21 (2002) 3317–3326.
[6] R. Chiesa, D.A. Harris, Prion diseases: what is the neurotoxic molecule? Neurobiol. Dis. 8 (2001) 743–763.
[7] E. Cohen, A. Taraboulos, Scrapie-like prion protein accumulates in aggresomes of cyclosporin A-treated cells, EMBO J. 22 (2003) 404–417.
[8] B. Drisaldi, R.S. Stewart, C. Adles, L.R. Stewart, E. Quaglio, E. Biasini, L. Fioriti, R. Chiesa, D.A. Harris, Mutant PrP is delayed in its exit from the endoplasmic reticulum, but neither wild-type nor mutant PrP undergoes retrotranslocation prior to proteasomal degradation, J. Biol. Chem. 278 (2003) 21732–21743.
[9] M.E. Figueiredo-Pereira, K.A. Berg, S. Wilk, A new inhibitor of the chymotrypsin-like activity of the multicatalytic proteinase complex (20S proteasome) induces accumulation of ubiquitin-protein conjugates in a neuronal cell, J. Neurochem. 63 (1994) 1578–1581.
[10] G. Forloni, N. Angeretti, R. Chiesa, E. Monzani, M. Salmona, O. Bugiani, F. Tagliavini, Neurotoxicity of a prion protein fragment, Nature 362 (1993) 543–546.
[11] T. Jin, Y. Gu, G. Zanusso, M. Sy, A. Kumar, M. Cohen, P. Gambetti, N. Singh, The chaperone protein BiP binds to a mutant prion protein and mediates its degradation by the proteasome, J. Biol. Chem. 275 (2000) 38699–38704.
[12] R.R. Kopito, ER quality control: the cytoplasmic connection, Cell 88 (1997) 427–430.
[13] C. Kuwahara, A.M. Takeuchi, T. Nishimura, K. Haraguchi, A. Kubosaki, Y. Matsumoto, K. Saeki, T. Yokoyama, S. Itohara, T. Onodera, Prions prevent neuronal cell-line death, Nature 400 (1999) 225–226.
[14] J. Ma, S. Lindquist, Wild-type and PrP and a mutant associated with prion disease are subject to retrograde transport and proteasome degradation, Proc. Natl. Acad. Sci. U.S.A. 98 (2001) 14955–14960.
[15] J. Ma, R. Wollmann, S. Lindquist, Neurotoxicity and neurodegeneration when PrP accumulates in the cytosol, Science 298 (2002) 1781–1785.
[16] G. Mallucci, A. Dickinson, J. Linehan, P.C. Klohn, S. Brandner, J. Collinge, Depleting neuronal PrP in prion infection prevents disease and reverses spongiosis, Science 302 (2003) 871–874.
[17] M. Marella, J. Chabry, Neurons and astrocytes respond to prion infection by inducing microglia recruitment, J. Neurosci. 24 (2004) 620–627.
[18] C.N. O'Donovan, D. Tobin, T.G. Cotter, Prion protein fragment PrP-(106–126) induces apoptosis via mitochondrial disruption in human neuronal SH-SY5Y cells, J. Biol. Chem. 276 (2001) 43516–43523.
[19] E. Paitel, C. Alves da Costa, D. Vilette, J. Grassi, F. Checler, Overexpression of PrPc triggers caspase 3 activation: potentiation by proteasome inhibitors and blockade by anti-PrP antibodies, J. Neurochem. 83 (2002) 1208–1214.
[20] E. Paitel, R. Fahraeus, F. Checler, Cellular prion protein sensitizes neurons to apoptotic stimuli through Mdm2-regulated and p53-dependent caspase 3-like activation, J. Biol. Chem. 278 (2003) 10061–10066.
[21] V. Perrier, K. Kaneko, J. Safar, J. Vergara, P. Tremblay, S.J. DeArmond, F.E. Cohen, S.B. Prusiner, A.C. Wallace, Dominant-negative inhibition of prion replication in transgenic mice, Proc. Natl. Acad. Sci. U.S.A. 99 (2002) 13079–13084.
[22] T. Pillot, B. Drouet, M. Pincon-Raymond, J. Vandekerckhove, M. Rosseneu, J. Chambaz, A nonfibrillar form of the fusogenic prion protein fragment [118-135] induces apoptotic cell death in rat cortical neurons, J. Neurochem. 75 (2000) 2298–2308.
[23] R.K. Plemper, D.H. Wolf, Retrograde protein translocation: ERADication of secretory proteins in health and disease, Trends Biochem. Sci. 24 (1999) 266–270.
[24] S.B. Prusiner, Prions, Proc. Natl. Acad. Sci. U.S.A. 95 (1998) 13363–13383.
[25] J. Schultz, A. Schwarz, S. Neidhold, M. Burwinkel, C. Riemer, D. Simon, M. Kopf, M. Otto, M. Baier, Role of interleukin-1 in prion disease-associated astrocyte activation, Am. J. Pathol. 165 (2004) 671–678.
[26] L. Solforosi, J.R. Criado, D.B. McGavern, S. Wirz, M. Sanchez-Alavez, S. Sugama, L.A. DeGiorgio, B.T. Volpe, E. Wiseman, G. Abalos, E. Masliah, D. Gilden, M.B. Oldstone, B. Conti, R.A. Williamson, Cross-linking cellular prion protein triggers neuronal apoptosis in vivo, Science 303 (2004) 1514–1516.
[27] G.C. Telling, T. Haga, M. Torchia, P. Tremblay, S.J. DeArmond, S.B. Prusiner, Interactions between wild-type and mutant prion proteins modulate neurodegeneration in transgenic mice, Genes Dev. 10 (1996) 1736–1750.
[28] D. Westaway, J. Cayetano-Canlas, D. Groth, D. Foster, S.-L. Yang, M. Torchia, G.A. Carlson, S.B. Prusiner, Degeneration of skeletal muscle, peripheral nerves, and the central nervous system in transgenic mice overexpressing wild-type prion proteins, Cell 76 (1994) 117–129.
[29] Y. Yedidia, L. Horonchik, S. Tzaban, A. Yanai, A. Taraboulos, Proteasomes and ubiquitin are involved in the turnover of the wild-type prion protein, EMBO J 20 (2001) 5383–5391.
[30] G. Zanusso, R.B. Petersen, T. Jin, Y. Jing, R. Kanoush, S. Ferrari, P. Gambetti, N. Singh, Proteasomal degradation and N-terminal protease resistance of the codon 145 mutant prion protein, J. Biol. Chem. 274 (1999) 23396–23404.
[31] H. Zhou, F. Cao, Z. Wang, Z.X. Yu, H.P. Nguyen, J. Evans, S.H. Li, X.J. Li, Huntingtin forms toxic $NH_2$-terminal fragment complexes that are promoted by the age-dependent decrease in proteasome activity, J. Cell Biol. 163 (2003) 109–118.

Available online at www.sciencedirect.com
SCIENCE DIRECT®
Biochemical and Biophysical Research Communications 327 (2005) 894–899
BBRC
www.elsevier.com/locate/ybbrc

# Prion protein with Y145STOP mutation induces mitochondria-mediated apoptosis and PrP-containing deposits in vitro

Naomi S. Hachiya[a,b], Kota Watanabe[a,b], Makiko Y. Kawabata[a,b], Akiko Jozuka[a,b], Yoshimichi Kozuka[c], Yuji Sakasegawa[a], Kiyotoshi Kaneko[a,b,*]

[a] *Department of Cortical Function Disorders, National Institute of Neuroscience (NIN), National Center of Neurology and Psychiatry (NCNP), Kodaira, Tokyo 187-8502, Japan*
[b] *Core Research for Evolutional Science and Technology (CREST), Japan Science and Technology Corporation, Japan*
[c] *Department of Ultrastructural Research, National Institute of Neuroscience (NIN), National Center of Neurology and Psychiatry (NCNP), Kodaira, Tokyo 187-8502, Japan*

Received 2 December 2004
Available online 29 December 2004

**Abstract**

A pathogenic truncation of an amber mutation at codon 145 (Y145STOP) in Gerstmann–Straussler–Scheinker disease (GSS) was investigated through the real-time imaging in living cells, by utilizing GFP-PrP constructs. GFP-PrP(1–144) exhibited an aberrant localization to mitochondria in mouse neuroblastoma neuro2a (N2a) and HpL3-4 cells, a hippocampal cell line established from *prnp* gene-ablated mice, whereas full-length GFP-PrP did not. The aberrant mitochondrial localization was also confirmed by Western blot analysis. Since GFP-PrP(1–121), as previously reported, and full-length GFP-PrP do not exhibit such mitochondrial localization, the mitochondrial localization of GFP-PrP(1–144) requires not only PrP residues 121–144 (in human sequence) but also COOH-terminal truncation in the current experimental condition. Subsequently, the GFP-PrP(1–144) induced a change in the mitochondrial innermembrane potential ($\Delta\Psi_m$), release of cytochrome *c* from the intermembrane space into the cytosol, and DNA fragmentation in these cells. Non-fluorescent PrP(1–144) also induced the DNA fragmentation in N2a and HpL3-4 cells after the proteasomal inhibition. These data may provide clues as to the molecular mechanism of the neurotoxic property of Y145STOP mutation. Furthermore, immunoelectron microscopy revealed numerous electron-dense deposits in mitochondria clusters of GFP-PrP(1–144)-transfected N2a cells, whereas no deposit was detected in the cells transfected with full-length GFP-PrP. Co-localization of GFP/PrP-immunogold particles with porin-immunogold particles as a mitochondrial marker was observed in such electron-dense vesicular foci, resembling those found in autophagic vacuoles forming secondary lysosomes. Whether such electron-dense deposits may serve as a seed for the growth of amyloid plaques, a characteristic feature of GSS with Y145STOP, awaits further investigations.


*Keywords:* Cellular prion protein; Green fluorescent protein; PrP Y145STOP mutation; Mitochondria-mediated apoptosis; PrP-containing deposits

Prion protein (PrP) consists of two isoforms, one is a host-encoded cellular isoform ($PrP^C$) and the other is an abnormal protease-resistant pathogenic isoform ($PrP^{Sc}$), of which the latter is a causative agent of prion disease. $PrP^{Sc}$ stimulates the conversion of $PrP^C$ into nascent $PrP^{Sc}$, and the accumulation of $PrP^{Sc}$ leads to central nervous system dysfunction and neuronal degeneration both in humans and animals [1]. The human prion diseases include kuru, Creutzfeldt–Jakob disease, Gerstmann–Straussler–Scheinker disease (GSS), and fatal familial insomnia [2,3].

* Corresponding author. Fax: +81 42 346 1748.
*E-mail address:* kaneko@ncnp.go.jp (K. Kaneko).

0006-291X/$ - see front matter © 2004 Elsevier Inc. All rights reserved.
doi:10.1016/j.bbrc.2004.12.079

We previously demonstrated the microtubule-associated intracellular localization of the $NH_2$-terminal fluorescent $PrP^C$ fragment [4] in mouse neuroblastoma neuro2a (N2a) and HpL3-4 cells, a hippocampal cell line established from *prnp* gene-ablated mice [5], by utilizing double-labeled $PrP^C$. We detected $NH_2$-terminally fluorescent-tagged $PrP^C$ predominantly in the intracellular compartments, COOH-terminally fluorescent-tagged $PrP^C$ mostly at the cell surface membranes overlapping with lipid rafts, and $PrP^C$ in full length with the merged color in Golgi compartments. Truncated $PrP^C$ with the amino acid residues 1–121, 1–111, and 1–91 in mouse PrP exhibited a proper distribution profile. Following real-time imaging analysis with GFP-$PrP^C$ revealed that the discrete $NH_2$-terminal amino acid residues are indispensable for the anterograde and the retrograde intracellular movements of GFP-$PrP^C$ [6]. Consistent with our reports, other groups also found the GFP-tagged version of $PrP^C$ to be properly anchored at the cell surface and its distribution pattern to be similar to that of the endogenous $PrP^C$, with labeling at the plasma membrane and in an intracellular perinuclear compartment [7–11].

Meanwhile, a pathogenic truncation of an amber mutation at codon 145 (Y145STOP) in the *prnp* gene, which was identified in a Japanese patient with GSS [12], came to our notice. The Y145STOP in human *prnp* gene corresponds to Y144STOP in mouse *prnp* gene which yields a product, mouse PrP(1–143) but hereafter designated PrP(1–144), and results in intracellular accumulation if proteasomal degradation is impaired [13]. Until now, its precise subcellular localization and relevance to the neurotoxic property have not been well characterized. Hence, GFP version of PrP(1–144) transgene was constructed and transfected in two independent cell lines, N2a and HpL3-4 cells.

Here we demonstrate for the first time that GFP-PrP(1–144) exhibited an aberrant mitochondrial localization accompanied by the depolarization of mitochondrial innermembrane, cytochrome *c* release in the cytosol, DNA fragmentation, and the formation of numerous PrP-containing deposits in intracellular vacuoles resembling secondary lysosomes.

## Materials and methods

*Construction of GFP-PrP and GFP-PrP(1–144).* GFP-PrP constructs were made as previously described [4,6], and the resulted plasmid was designated pSPOX-MHM2PrP::GFP. The mutant was amplified by PCR from the pSPOX-MHM2PrP::GFP (for amino acid residues Δ144–230 in mouse PrP) [4,6], digested with *Bam*HI and *Xho*I, and replaced with the *Bam*HI–*Xho*I fragment of pSPOX-MHM2PrP::GFP [14]. Non-fluorescent PrP constructs were made from the pSPOX-MHM2PrP [14]. The resulted plasmid was verified by direct DNA sequencing.

*Antibodies and drugs.* Antibody K3 against $PrP^C$ was rabbit polyclonal sera raised against N-terminal PrP peptides corresponding to residues 76–90 in mouse PrP. Anti-cytochrome *c* and anti-porin were purchased from BD Biosciences. Anti-Hsc70 and anti-BiP were purchased from Stressgen Biotechnologies. Anti-GFP was purchased from Sigma. Mitotracker Red CMXRos was purchased from Molecular Probes. Lactacystin, ALLN, and MG132 were purchased from Sigma. The mitochondrial innermembrane potential ($\Delta\Psi_m$) detection kit was purchased from Trevigen. DNA fragmentation was measured by TUNEL (APO-BrdU TUNEL assay kit (Molecular Probes)), which was performed according to the manufacturer's instructions before being visualized with a Delta-Vision microscopy system (Applied Precision), and out-of-focus images were removed by interactive deconvolution. Antibodies were used at 1:1000 (Western blotting) or 1:100 (immunoelectron microscopy) unless otherwise noted. For immunoelectron microscopy, 10 and 20 nm golds were purchased from DAKO.

*Cell cultures, DNA transfection, and drug treatments.* Mouse N2a cells were obtained from American Tissue Culture Collection, and HpL3-4 cells were provided by Dr. T. Onodera (the University of Tokyo). Cells were grown and maintained at 37 °C in MEM supplemented with 10% fetal bovine serum. N2a and HpL3-4 cells were transiently transfected with each construct using a DNA transfection kit (Lipofectamin, Gibco-BRL). Western blot analyses were performed as described [14]. To inhibit proteasomal function, N2a or HpL3-4 cells were treated with 10 μM lactacystin, ALLN, or MG132 for 3.5 h at 37 °C.

*Preparation of mitochondrial, microsomal, and cytosolic fractions [15].* Cells were homogenized with 9 volumes of mitochondrial buffer (220 mM mannitol, 70 mM sucrose, 10 mM Hepes–KOH, pH 7.4, and 0.1 mM EDTA) and centrifuged at 700*g* for 5 min at 4 °C, and the supernatant was further centrifuged at 5000*g* for 10 min at 4 °C. The supernatant was used as a post-mitochondrial supernatant. The resulted pellet was washed three times with mitochondrial buffer, resuspended in 9 volumes of the same buffer, and then centrifuged at 2000*g* for 2 min at 4 °C followed by 5000*g* for 8 min at 4 °C. The pellet was resuspended in 9 volumes of the same buffer and then centrifuged at 5000*g* for 10 min at 4 °C. The final pellet was recovered and stored on ice until use (mitochondrial fraction). The post-mitochondrial supernatant was further centrifuged at 100,000*g* for 1 h at 4 °C, and the supernatant was used as cytosolic fraction, and the pellet was resuspended in mitochondrial buffer (microsomal fraction). Western blots were performed at 5 μg total protein/lane.

*Real-time imaging.* To observe living cells, cells were cultured on glass-bottomed dishes (Matsunami) for 24–48 h after the DNA transfection. To visualize mitochondria, cells were incubated for 10 min at 37 °C with Mitotracker Red CMXRos at desired concentrations. Images of cells were collected with a Delta Vision Microscopy System (Applied Precision) equipped with an Olympus IX70.

## Results

The intracellular localization of fluorescent $PrP^C$ was investigated through the real-time imaging in living cells by utilizing GFP-PrP constructs. It was investigated in N2a cells that can be infected with $PrP^{Sc}$ [16] and has been widely used for studies in the $PrP^C$ metabolism, as well as in HpL3-4 cells, a hippocampal cell line established from *prnp* gene-ablated mice [5].

GFP-PrP(1–144) exhibited an aberrant localization to mitochondria, as demonstrated by its colocalization with the mitochondrial-specific molecule, Mitotracker, in N2a cells (Fig. 1A, upper panels) and HpL3-4 cells (Fig. 1A, lower panels), whereas full-length GFP-PrP did not. Previously, we also demonstrated that GFP-

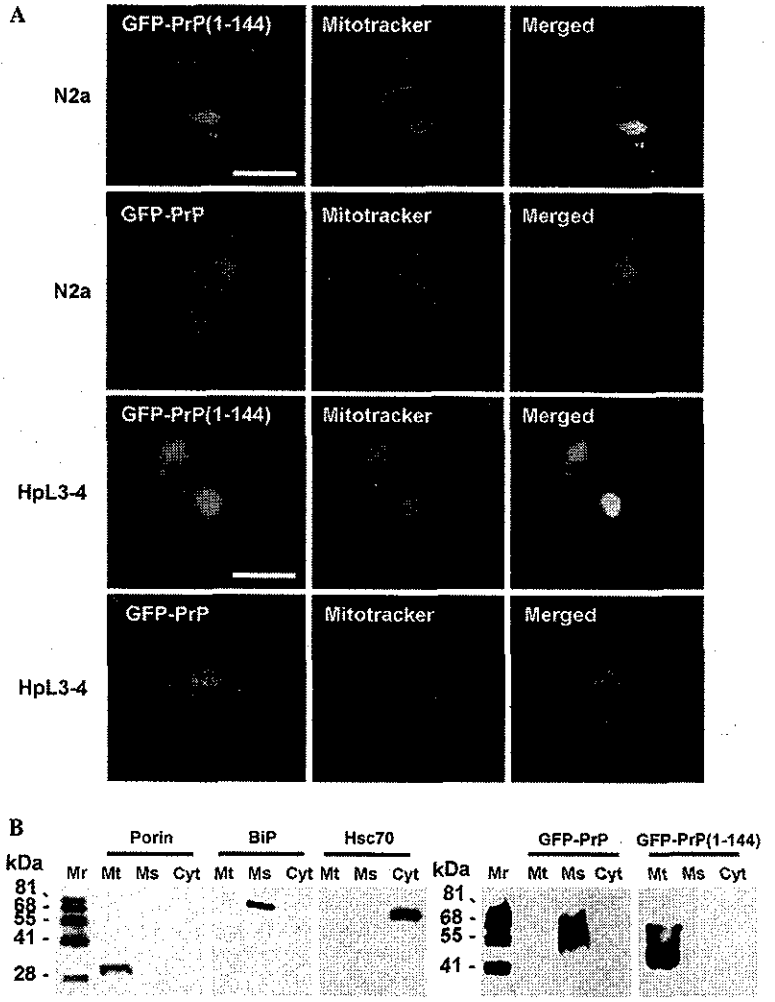


Fig. 1. Mitochondrial localization of GFP-PrP(1–144). GFP-PrP(1–144) exhibits aberrant localization in N2a cells, whereas full-length GFP-PrP does not. (A) GFP-PrP$^C$ localization. Full-length GFP-PrP and GFP-PrP(1–144) constructs were made and transfected in N2a (upper panels) and HpL3-4 cells (lower panels). Scale bars = 8 μm. (B) Western blot analysis with anti-GFP antibody. Anti-porin antibody was used as a mitochondrial (Mt) marker, anti-BiP antibody was used as a microsome (Ms) marker, and anti-Hsc70 antibody was used as a cytosolic (Cyt) marker. Mr, molecular weight marker.

PrP(1–121) does not exhibit such mitochondrial localization [4]. Thus, the mitochondrial localization of GFP-PrP(1–144) requires not only PrP residues 121–144 (in human sequence) but also COOH-terminal truncation in the current experimental condition, regardless of whether endogenous full-length PrP$^C$ exists. The aberrant mitochondrial localization of GFP-PrP(1–144) was further confirmed by Western blot analysis using a subcellular fractionation method (Fig. 1B).

Subsequently, the GFP-PrP(1–144) induced the depolarization of mitochondrial innermembrane (a change in the $\Delta\Psi_m$) in N2a (Fig. 2A, upper panels) and HpL3-4 cells (Fig. 2A, lower panels), release of cytochrome *c* from the intermembrane space into the cytosol (Fig. 2B), and DNA fragmentation assessed by TUNEL in N2a (Fig. 2C, upper panels) and HpL3-4 cells (data not shown). The PrP(1–144) is normally degraded through the proteasomal pathway, but intracellular accumulation results if proteasomal degradation is impaired [13]. Therefore, we next set out to treat the non-fluorescent PrP(1–144)-transfected cells with proteasome inhibitors including lactacystin, ALLN, or MG132. After the lactacystin treatment, non-fluorescent PrP(1–144) induced the DNA fragmentation in N2a (Fig. 2C, lower panels) and HpL3-4 cells (data not shown). Treatment with ALLN or MG132 also exhibited similar results (data not shown). These observations are characteristic of the mitochondria-mediated apoptotic process. In contrast, none of these abnormalities was observed in N2a and HpL3-4 cells transfected with full-length GFP-PrP construct.

During these investigations, we noticed that GFP-PrP(1–144)-transfected N2a and HpL3-4 cells lost its normal mitochondrial configurations as if congregated predominantly in an intracellular perinuclear region. To further investigate the ultrastructural

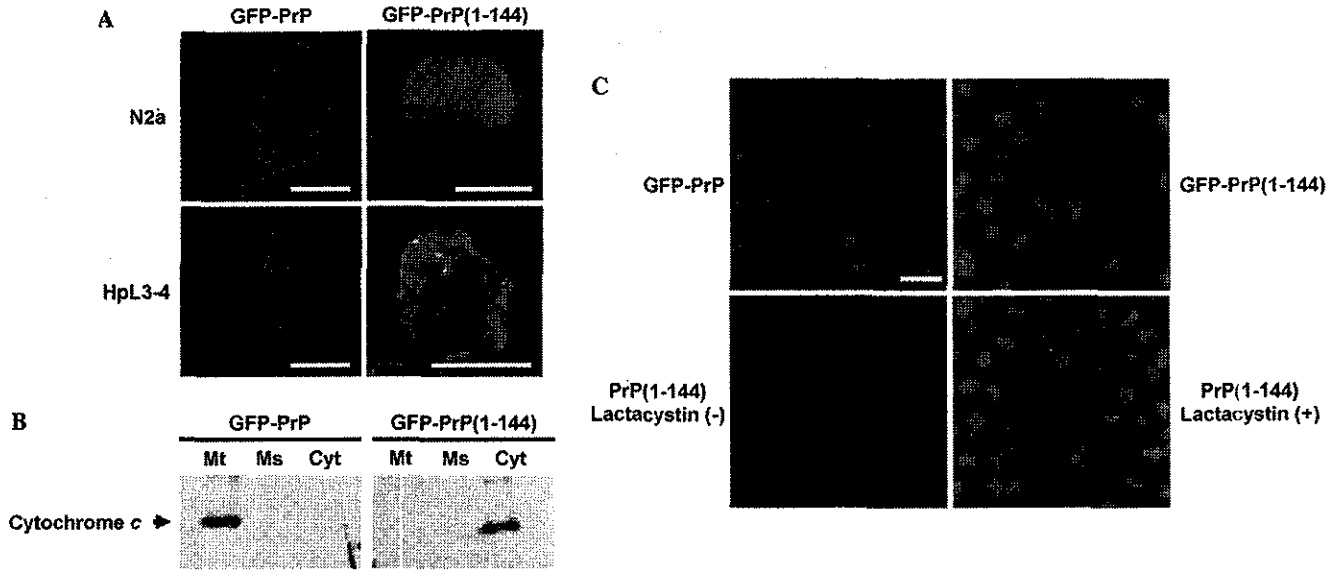


Fig. 2. Accumulation of GFP-PrP(1–144) induces mitochondria-mediated apoptosis. (A) Inactivation of the mitochondrial innermembrane potential ($\Delta\Psi_m$, red; active, green; inactive) in N2a (upper panels) and HpL3-4 (lower panels) cells transfected with GFP-PrP(1–144). Scale bars = 4 μm. (B) The release of cytochrome *c* from the mitochondria in N2a cells transfected with GFP-PrP(1–144). Mt, mitochondria fraction; Ms, microsome fraction; and Cyt, cytosolic fraction. The markers are the same as shown in Fig. 1B. (C) Upper panels: DNA fragmentations measured by TUNEL (red; negative, green; positive) are shown in N2a cells transfected with GFP-PrP(1–144). Lower panels: non-fluorescent PrP(1–144) transfected in N2a cells also exhibits the DNA fragmentation in a lactacystin-dependent manner. Scale bars = 15 μm.

morphology of these mitochondria, we next performed electron microscopy in N2a cells transfected with GFP-PrP(1–144) in comparison with full-length GFP-PrP.

As results, numerous electron-dense deposits were observed in mitochondrial clusters of the GFP-PrP(1–144)-transfected N2a cells, whereas none was detected in N2a cells transfected with full-length GFP-PrP (Fig. 3A). Some vesicles contained myelin-like figures resembling those found in autophagic vacuoles forming secondary lysosomes (Fig. 3B). Co-localization of PrP-immunogolds (Fig. 3C, left panel)/GFP-immunogolds (Fig. 3C, middle panel) with porin-immunogold particles as a mitochondrial marker (Fig. 3C, right panel) was observed in such electron-dense vesicular foci. Non-fluorescent PrP(1–144) also induced the same deposits after the proteasomal inhibition (data not shown).

## Discussion

The Y145STOP mutation at PrP residue 145 results in a heritable human prion disease, GSS-like disorder, with extensive PrP amyloid deposits in cerebral parenchyma and vessels [12,17]. The Y145STOP, which yields a product of PrP(1–144), lacks GPI-anchor and is normally degraded through the proteasomal pathway, and also results in intracellular accumulation if proteasomal degradation is impaired [13]. Most PrP(1–144) is degraded very rapidly by the proteasome-mediated pathway, and thus blockage of proteasomal degradation results in intracellular accumulation of PrP(1–144). From the current results, however, the GFP-tagged PrP(1–144) seems to be more metabolically stable, and therefore GFP-PrP(1–144) expression itself is sufficient to induce its intracellular accumulation. In fact, non-fluorescent PrP(1–144) required the treatment with proteasome inhibitors to exhibit the same features.

In this paper, we revealed for the first time the site of intracellular accumulation and the neurotoxic property of mutant $PrP^C$, Y145STOP, in a human GSS model. The GFP-PrP(1–144) exhibited an aberrant localization to mitochondria, and subsequent mitochondria-mediated apoptosis was induced. Misfolded $PrP^C$ is subjected to degradation by proteasomes, and accumulation of $PrP^C$ in the cytosol is strongly neurotoxic in transgenic mice [18] and cyclosporin A-treated cultured cells [19], and proteasome inhibitors increase $PrP^C$-like immunoreactivity and unmasked a basal caspase 3 activation [20]. Concomitant with decreased proteasomal activity, aberrant mitochondrial localization of $PrP^C$ followed by mitochondria-mediated neuronal apoptosis was also detected in aged transgenic mice overexpressing wild-type mouse $PrP^C$, but only after 520 days after birth [15]. These mice develop a spontaneous neurological dysfunction in an age-dependent manner [21,22]. Taken together, a $PrP^C$ load in the cytosol induces the mitochondrial localization of $PrP^C$ with subsequent mito-